

LUT UNIVERSITY
LUT School of Energy Systems
LUT Mechanical Engineering

Lassi Punkkinen

STRUCTURAL ANALYSIS AND OPTIMIZATION OF ASH HOPPER DESIGN

16.11.2021

Examiner(s): Professor Timo Björk
M.Sc. (Tech.) Timo Sorjonen

TIIVISTELMÄ

LUT-Yliopisto
LUT School of Energy Systems
LUT Kone

Lassi Punkkinen

Structural analysis and optimization of ash hopper design

Diplomityö

2021

93 sivua, 53 kuvaa, 14 taulukkoa ja 1 liite

Tarkastajat: Professori Timo Björk
DI Timo Sorjonen

Hakusanat: suppilo, levyrakenteet, jäykistetty levykenttä, optimointi

Tämän diplomityön tarkoituksena on tutkia ja kehittää kattilalaitoksen tuhkasuppiloiden mitoitusta ja rakennetta perehtyen nykyisiin suppilorakenteisiin sekä soveltaen teräsrakennes-standardeja. Tavoitteena on lisäksi suppiloiden valmistuskustannusten ja massan optimointi sekä laskennan yhtenäistäminen.

Toisin kuin kattilan painelaitteille, tuhkasuppiloille ei ole suoraa standardia, joka määräisi suppilon suunnittelua yksikäsitteisesti. Suppilon suunnittelukriteerit asetettiin soveltaen osaa Eurokoodi-standardeja sekä yleistä lujuusoppia. Kuormitukseen liittyvät vaatimukset tulevat osin standardeista sekä tuotekohtaisesti Valmetilta.

Tuhkasuppilo on hitsattu levyrakenne, jonka pääasiallisena kuormituksena on levyn normaalin suuntainen painekuorma. Työssä esitellään suppilorakenteiden laskentaan tarvittavaa perusteoriaa kuten jäykistettyjen levykenttien, jäykisteiden ja hitsien mitoitusta. Korkean lämpötilan huomioon ottaminen on myös oleellinen osa tuhkasuppiloiden tarkastelussa.

Suppilorakenteen lujuustarkastelu suoritettiin pääosin käyttäen FE-analyysiä. Lisäksi sovellettiin yksinkertaistettuja analyttisiä laskentakaavoja, joiden soveltuvuus varmistettiin vertailulla. Erilaisia rakenneratkaisuja vertailtiin tutkien esimerkkipiltoa. Rakennetta voitiin keventää yleisesti optimoimalla jäykisteiden paikoitusta, muokkaamalla rakenteen yksityiskohtia sekä vähentämällä hitsiliitoksia. Työn tuloksena laadittiin mitoitus työkalu tuhkasuppiloiden perusrakenteen määrittämiseksi. Työn lopussa pohditaan lisäksi mahdollisia jatkokehityskohteita sekä potentiaalisia parannusehdotuksia.

ABSTRACT

LUT University
LUT School of Energy Systems
LUT Mechanical Engineering

Lassi Punkkinen

Structural analysis and optimization of ash hopper design

Master's thesis

2021

93 pages, 53 figures, 14 tables and 1 appendix

Examiners: Professor Timo Björk
M. Sc. (Tech.) Timo Sorjonen

Keywords: hopper, plate structures, stiffened plate, optimization

The purpose of this thesis is to research and develop the design and dimensioning of boiler ash hoppers by analyzing existing hoppers and applying relevant steel structure standards. The goal is also to optimize the mass and manufacturing costs of hoppers and harmonize the calculation.

Unlike for pressure parts of the boiler, there is no direct standard that would set explicit design requirements for ash hoppers. The design criteria of the hopper were set by applying Eurocode-standards and basic strength of materials. The requirements related to loads are obtained partly from standards and product-specifically from Valmet.

Ash hopper is a welded plate structure that is mainly subjected to out-of-plane pressure loads. The thesis presents the basic theory needed in the calculation of hopper structures including the dimensioning of stiffened plates, stiffeners, and welds. Considering the high temperatures is also an important aspect in the analysis of ash hoppers.

The structural analysis of ash hoppers was primarily done with FE-analysis. Simplified analytical calculations were additionally applied and results were verified by comparison. Different design constructions were compared by analyzing an example hopper. The structure could be generally enhanced by optimizing the placement of stiffeners, modifying design details, and reducing the amount of welding. Based on the results of this thesis, a dimensioning tool was developed for determining the basic design parameters for ash hoppers. Future development ideas and potential improvement areas are discussed at the end of the thesis.

ACKNOWLEDGEMENTS

This Master's thesis was done for Valmet's boiler engineering department in Tampere. I would like to thank Valmet for an interesting concrete topic and Tuomas Etula for making this thesis possible. Thank you to Timo Sorjonen, Juha Ojanperä and Jukka Kattelus for valuable discussions and guidance during the thesis. I also want to thank Professor Timo Björk for the useful comments regarding the thesis and for the lessons taught during my years at LUT University. I am grateful for all the student years, and I would like to thank all the friends and family for the great times and support along the way.

Lassi Punkkinen

Tampere 16.11.2021

TABLE OF CONTENTS

TIIVISTELMÄ

ABSTRACT

ACKNOWLEDGEMENTS

TABLE OF CONTENTS

LIST OF SYMBOLS AND ABBREVIATIONS

1	INTRODUCTION	11
1.1	Ash hopper	12
1.2	Research problem	14
1.3	Objective and goals.....	15
1.4	Research methods	16
1.5	Framing	16
2	LOADS ACTING ON THE HOPPER	18
2.1	The dead weight of the structures	18
2.2	Ash load	18
2.3	Flue gas pressure.....	20
2.4	Temperatures	21
2.5	Partial safety factors and load combinations	21
3	DESIGN CRITERIA OF AN ASH HOPPER.....	23
3.1	Standards guiding the design of an ash hopper.....	23
3.2	Limit state design.....	27
3.2.1	Serviceability limit states.....	27
3.2.2	Ultimate limit states	28
3.3	Plates	29
3.4	Stiffeners	33
3.5	Effect of high temperatures on materials	42
3.5.1	Mechanical properties.....	42
3.5.2	Creep.....	44
3.6	Dimensioning of welds	46
3.7	Stability.....	51
3.7.1	Effect of temperature on the stability	54
3.8	Erosion, abrasion and corrosion.....	55
3.9	Design details.....	56

4	FE-ANALYSIS	57
4.1	Material.....	57
4.2	Geometry and elements	57
4.3	Loads and boundary conditions	58
5	ANALYSIS AND OPTIMIZATION OF THE DESIGN	59
5.1	Simplifications	59
5.2	Analysis and optimization of stiffened plates.....	61
5.3	Optimization of the design.....	69
6	DIMENSIONING TOOL	77
7	DISCUSSION	84
7.1	Most important factors defining the design and analysis	84
7.2	Design optimization.....	85
7.3	Dimensioning tool.....	86
7.4	Future development	87
8	CONCLUSION	90
	LIST OF REFERENCES	91
	APPENDICES	

Appendix I: Creep properties of pressure grade steels

LIST OF SYMBOLS AND ABBREVIATIONS

A	Cross-sectional area [mm ²]
a	Smaller side of plate segment [mm]
A_{prof}	Cross-section area of combination profile [mm ²]
A_{rod}	Pressure area for rod [mm ²]
A_w	Weld cross-section area [mm ²]
a_w	Weld throat thickness [mm]
b	Longer side of plate segment [mm]
b_t	Maximum horizontal width of the tie [mm]
b_0	Half of the stiffener span [mm]
B_{eff}	Effective width of plate flange on each side of stiffener [mm]
c	Maximum distance from the neutral axis [mm]
C_s	Shape factor for the tie cross-section
C_t	Load magnification factor
D	Plate flexural rigidity [Nmm]
d_y	Distance between components neutral axis in y-direction [mm]
d_z	Distance between components neutral axis in z-direction [mm]
E	Young's modulus [MPa]
f_{cr}	Critical buckling stress for the relevant buckling mode [MPa]
$f_{cr,\theta}$	Critical buckling stress for the relevant buckling mode at a temperature [MPa]
$F_{iw,Ed}$	Intermittent weld shear force per length [N/mm]
f_u	Nominal ultimate tensile strength of the weaker part [MPa]
$F_{w,Ed}$	Weld shear force per length [N/mm]
$F_{w,Rd}$	Design weld resistance per unit length [N/mm]
$f_{y,Ed}$	Design strength [MPa]
f_y	Yield strength [MPa]
$f_{y,\theta}$	Yield strength at temperature [MPa]
$f_{e,1.0}$	Strength for 1% plastic creep [MPa]
g	Gravitational acceleration [m/s ²]
$G_{k,j}$	Design value of permanent action
H	Total height of hopper [mm]

I_y	Second moment of area around y-axis [mm ⁴]
I_z	Second moment of area around z-axis [mm ⁴]
k_1, k_2, k_3	Factors for deflection
$k_{E,\theta}$	Reduction factor to the linear elastic range
k_L	Loading state factor
$k_{y,\theta}$	Reduction factor for yield strength of steel at a temperature
k_w	Coefficient for plate deflection
$k_{\sigma bx}$	Coefficient for plate bending stress around x-axis
$k_{\sigma by}$	Coefficient for plate bending stress around y-axis
L_1, L_2	Intermittent weld gap [mm]
L_e	Effective length of stiffener [mm]
L_n	Buckling length of member [mm]
L_{stiff}	Length of stiffener in a plate segment [mm]
L_w	Length of weld [mm]
M_{Ed}	Tension rod bending moment [Nmm]
M_{max}	Maximum bending moment [Nmm]
$N_{b,fi,Rd}$	Buckling resistance of the member at temperature [N]
$N_{b,Rd}$	Buckling resistance of the member [N]
N_{cr}	Elastic critical force for the relevant buckling mode [N]
$N_{c,Ed}$	Design value of compressive force [N]
N_{Ed}	Tension rod axial force [N]
n_{ew}	Effective width factor
P	Design value of prestressing action
p_{ash}	Ash hydrostatic pressure [MPa]
p_{fg}	Flue gas pressure [MPa]
p_{nf}	Normal pressure of ash particles [MPa]
p_{tf}	Friction traction of ash particles [MPa]
p_v	Vertical pressure within the stored material at the tie level [MPa]
q	Line load [N/mm]
Q	Statical moment of area [mm ³]
q_{Ed}	Design value of uniformly distributed load [MPa]
$Q_{k,1}$	Design value of variable action
q_t	Force per unit length of tie [N/mm]

$R_{m,c}$	Creep rupture strength [MPa]
$R_{p0.2}$	Minimum 0.2 % proof strength [MPa]
S	Shear force [N]
t	Plate thickness [mm]
ν	Poisson's ratio
w	Plate deflection [mm]
W	Section modulus [mm ³]
y_0	Center of area in y-axis [mm]
z	Coordinate along the height [mm]
z_0	Center of area in z-axis [mm]
α_{wall}	Wall angle [°]
α	Imperfection factor
β	Effective width factor
β_t	Tie location factor
β_w	Correlation factor dependent on the steel grade/filler metal
$\gamma_{G,j}$	Partial factor for permanent actions
$\gamma_{M,fi}$	Partial safety factor for resistance of members, at temperature
γ_{M1}	Partial safety factor for resistance of members
γ_{M2}	Material partial safety factor
γ_P	Partial factor for prestressing actions
$\gamma_{Q,1}$	Partial factor for variable actions
δ_{max}	Maximum lateral deflection [mm]
δ_{stiff}	Stiffener deflection [mm]
Δt_a	Wear allowance [mm]
ε	Coefficient for effective width factor
κ	Factor for calculation of effective width
$\bar{\lambda}$	Non-dimensional slenderness
$\bar{\lambda}_\theta$	Non-dimensional slenderness at temperature
ξ_j	Reduction factor for unfavorable permanent actions
ρ	Material density [kg/m ³]
σ_\perp	Normal stress perpendicular to the throat [MPa]
$\sigma_{bx,Ed}$	Bending stress around x-axis [MPa]
$\sigma_{by,Ed}$	Bending stress around y-axis [MPa]

$\sigma_{eq,Ed}$	Equivalent von Mises design stress [MPa]
σ_{stiff}	Bending stress of stiffener [MPa]
σ_y	Y-normal stress [MPa]
σ_z	Z-normal stress [MPa]
$\tau_{//}$	Shear stress parallel to the axis of the weld [MPa]
τ_{\perp}	Shear stress perpendicular to the axis of the weld [MPa]
τ_{xy}	Shear stress between components [MPa]
τ_{yz}	In-plane shear stress of plate [MPa]
χ	Reduction factor for the relevant buckling curve
χ_{fi}	Reduction factor for the relevant buckling curve at temperature
$\psi_{0,i}$	Reduction factor for accompanying variable actions
Φ	Intermediate factor for determining buckling reduction factor
Φ_{θ}	Intermediate factor for determining buckling reduction factor at temperature
BFB	Bubbling fluidized bed boiler
CFB	Circulating fluidized bed boiler
EC3	Eurocode 3
FEA	Finite element analysis
GNA	Geometrically non-linear analysis
LA	Linear analysis
LBA	Linear buckling analysis
NFPA	National fire protection association
RB	Recovery boiler
SLS	Serviceability limit state
ULS	Ultimate limit state

1 INTRODUCTION

Valmet is one of the global leaders in providing solutions and service for the paper, pulp and energy industries. This master's thesis is done for the boiler engineering department in Valmet's pulp and energy business line. The business line's main products can be divided into three main categories: pulp production, energy production and biomass conversion technologies. The boiler engineering department located in Tampere is responsible for the design and development of the boilers, gasifiers, and related structures.

Valmet produces three main boiler types: Valmet BFB (bubbling fluidized bed) Boiler, Valmet CFB (circulating fluidized bed) Boiler and Valmet Recovery Boiler (RB). Figure 1 presents the concepts of the main boiler types. BFB and CFB boilers can use various types of solid fuels like biomass, coal, wood products and waste. Black liquor is burned in a recovery boiler to produce energy and to recover chemicals for further use in the mill plant. The basic working principle of the boilers is similar, fuel is burned in the furnace to generate steam from circulating water and then the hot steam is used for producing electricity and heat. Burning a fuel always generates ash and it needs to be removed via ash handling system in a boiler. The ash is collected by various ash hoppers located within the ash handling and flue gas systems. Collected ash is then conveyed to fly ash silos for storage and transportation.

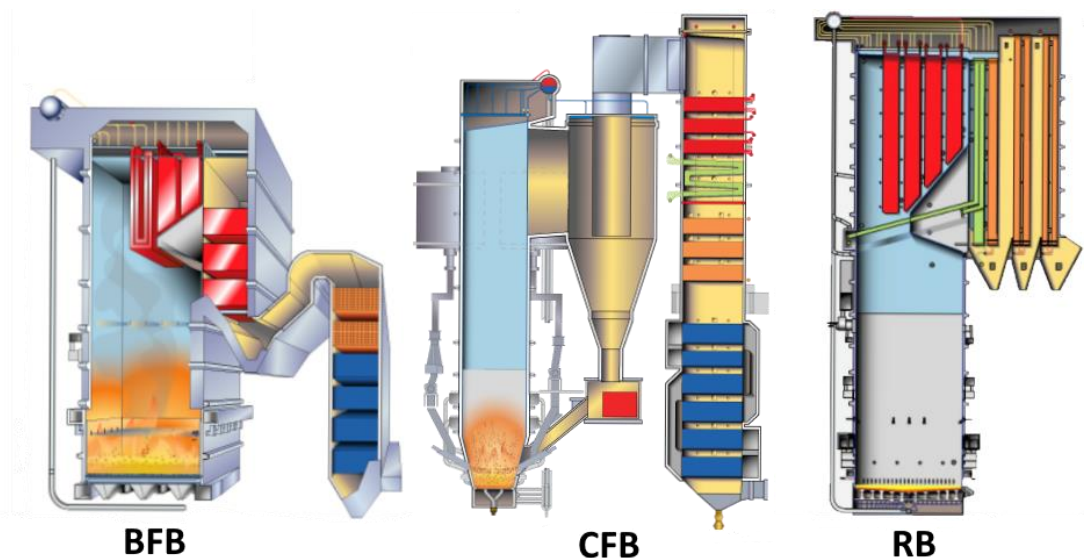


Figure 1. Boiler types (Valmet MyAcademy).

1.1 Ash hopper

Ash hoppers are part of the ash handling system in boilers, and they can also be considered as components in the flue gas system since the flue gases flow through the hoppers. There are multiple ash hoppers within the boiler as the ash is collected from several points. Hoppers below the filters in the flue gas cleaning system collect the majority of the total ash. Additionally, there are ash hoppers in the backpass before the flue gas cleaning system. These hoppers collect only a small portion of the total ash, but they are a critical component for the functionality and due to demanding conditions. These hoppers are the main focus of this thesis. The ash handling system especially in BFB and CFB boilers share similar design and components. Figure 2 presents the main components of an example CFB boiler ash handling and flue gas systems.

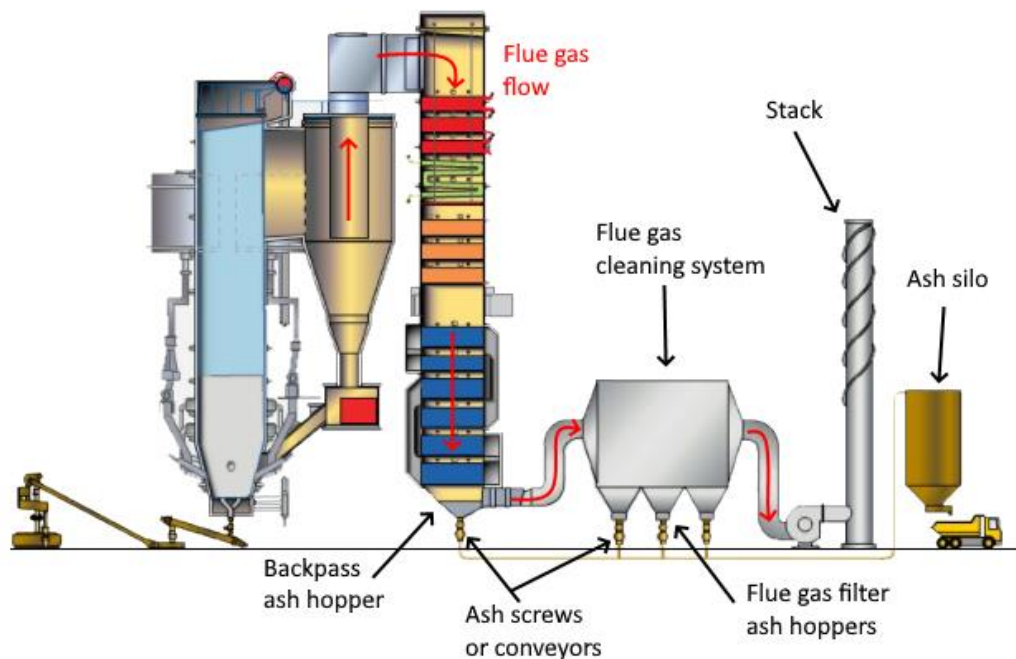


Figure 2. Example CFB boiler main components of ash handling system (Valmet MyAcademy).

The main purpose of the hopper is to collect the dropping ash particles from surfaces and out of flue gas. Flue gas flows through the hopper and into the flue gas duct, while some ash particles drop down onto the hopper. Ash flowing with flue gas is referred as fly ash. Flue gas temperatures vary based on the boiler type, configuration, and location but can be up to 550 °C when passing through the hopper. Ash hoppers are insulated from the outside with temperature-resistant mineral wool and rubber mats.

Ash hopper design changes based on the configuration, type and overall size of the boiler. For this research and optimization, one general type of hopper design and configuration was chosen. The basic design of the hopper is kept uniform, but the scale is varied. Top feeding hopper with the flue gas duct located on the side of the hopper was chosen as the focus. Variation of this type of hopper can be found in various configurations but usually in the backpass of CFB or BFB boiler. This type of hopper is generally the most demanding to design as it needs to be the largest in size and is subjected to the highest temperatures. The hoppers below the flue gas filters are different in design and are not specifically considered, but the same rules are applicable.

Ash hopper is a rectangular-shaped plate structure. It has a pyramidal bottom part and rectangular or slightly pyramidal top part. Overall dimensions vary but generally hopper width and depth are 2 – 20 m and the height 2 – 6 m. Typical plate thicknesses vary between 4 - 15 mm. The hopper walls are stiffened by outside horizontal stiffeners and vertically orientated inside stiffeners along the walls. Typical stiffeners used are flat bars, L-bars and U-beams. Additionally, whole plate walls are stiffened by the inside tension rods. Tension rods connect the walls and add overall rigidity. One sidewall of the hopper has a cut-out for the flue gas duct and the duct is attached by welding. Ash hopper is a part of the flue gas system and it must be gastight, so all joints in the structure are done by welding. Figure 3 presents an example ash hopper and related main components.

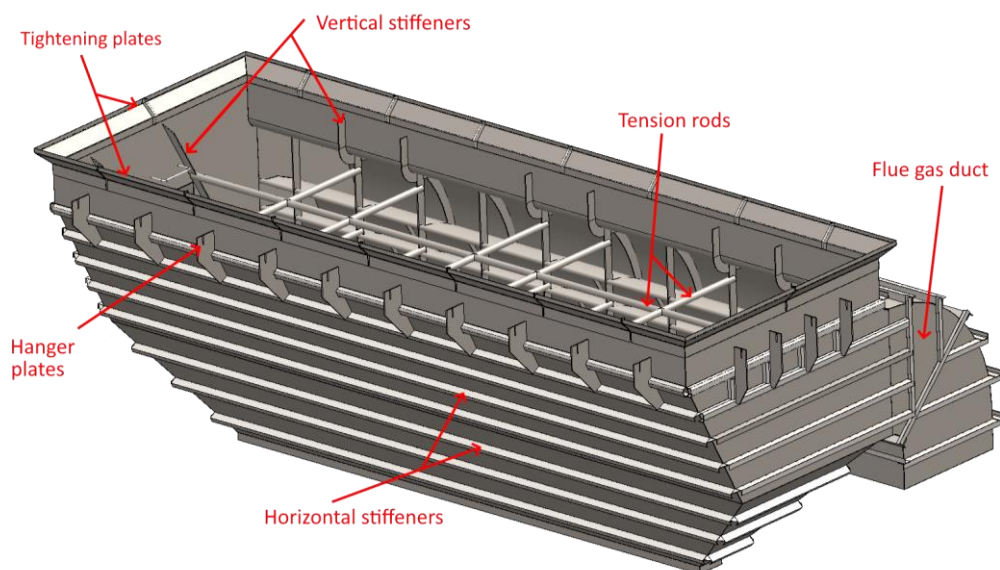


Figure 3. Example ash hopper and its main components.

Hopper is mainly loaded by dead weights, ash load and flue gas pressure. There are different options for the support constructions of hoppers, but figure 3 presents a hopper attached by hanger plates. Hanger plates are welded to the corresponding attachment plates above. Additionally, the top edge of the hopper is welded all around by the tightening plates to ensure a gastight seal. Ash screw or conveyor is attached to the bottom of the hopper to transport the ash into fly ash silos. The conveying system is hung from the hopper and typically has no separate supports beneath.

Ash hopper is usually too large to be transported as a whole to the site, so it cannot be fully fabricated at the workshop. Prefabricated blocks are prepared at a workshop and then packed for transportation. Blocks can be full or partial wall sections with welded stiffeners. Final assembly is then done at the site by combining and welding the prefabricated blocks together. Final fabrication of ash hopper on the site sets special challenges for assembly accuracy and easy manufacturability.

1.2 Research problem

Ash hoppers are designed project-specific while basing the design on previously produced hoppers and the design features are scaled up or down according to the reference. However, there are always differences between the hopper designs that require iteration and analyzing every hopper in detail is a tedious process that takes time and resources. Valmet has generated its own design instructions and calculation sheets for various boiler components, but ash hoppers do not have separate instructions yet.

The challenge is the wide range in the scale of the hoppers. Comparing the largest hopper, the dimensions can be up to 5 times of a small hopper. While the basic design remains mostly the same, specifically the need for stiffening increases greatly in larger plate areas. This increases the demands for the whole design. With such a variable scale, it is difficult to create optimum solutions for the range of designs. Even bigger boilers are also produced all the time and consequently, larger ash hoppers are then required. The highest possible savings in design, manufacturing and material costs are available in the largest structures, but requirements for the design are also the highest.

1.3 Objective and goals

The purpose of this thesis is to research and improve the design and dimensioning of ash hopper structures. Then the objective is to optimize material usage and manufacturing costs. Previous ash hoppers and calculations are studied along with related steel structure standards. The current design features can be altered, but the overall construction will remain mostly unchanged. The most important optimizable parameters are the determination of the stiffener layout and choosing the stiffener profiles. Welding is a major part of the hopper assembly and it is tried to be minimized to reduce manufacturing time and costs.

After analyzing and enhancing the overall design, the goal is to generate a dimensioning tool for project-specific ash hopper design. Given input data are the general dimensions of the hopper and the load data. The tool should provide the basic parameters for the design of the hopper based on the structural criteria. The list of parameters includes:

- Material recommendations
- Basic plate thicknesses
- The layout of horizontal and vertical stiffeners
- Stiffener profiles
- Placement of tension rods and profiles
- Design of welds
- Number of hanger plates

The tools should be easy and simple to use, and it is mainly intended for design engineers. The structural design that fulfills the dimensioning criteria should be obtained without detailed analysis by a structural engineer. Possible special cases that do not correspond to the base structure of the studied hopper will be checked separately. Another objective of the dimensioning tool is to generalize the hopper details. Although hoppers will always be designed project-specific, certain design features are uniform. In addition to generalizing the design, the aim is to standardize calculation with Eurocode practices. Eurocodes don't provide a direct guide for this special application, but multiple standards are reviewed and applied. Other sources and standards are also used.

1.4 Research methods

Research begins by studying existing ash hoppers and their design. Meetings and discussions with related design and structural engineers are utilized to gather possible improvement ideas. The manufacturing and assembly of hoppers is reviewed along with comments from practice. The previous structural analysis reports are studied to discover basic practices and possible problem areas in the analysis of previous ash hoppers. The goal is to develop the calculation methods and old calculations and reports are used just for reference.

Literature and standards relevant to ash hopper structures are reviewed. There is no direct design standard for an ash hopper, so the review is compiled using different standards and sources. The aim is to base the analysis mostly on EC3 (Eurocode 3) to uniform the practices. Literature and design standards are researched to combine the needed theory and equations for the calculations. Additionally, Valmet's own design instructions and material specifications are utilized in defining the design criteria. Other product-specific information is obtained from Valmet. Previous research on related topics is also utilized as the reference for the analysis.

Both analytical and numerical calculation methods will be used in the analysis of the ash hopper. Comparison between these results is used to verify the accuracy and reliability. Finite element analysis (FEA) is used as the numerical calculation tool and analytical equations for calculation are obtained from relevant Eurocodes and basic strength of materials. Analytical calculations require simplifying the problem into a suitable form and analyzing structural members separately and FEA is then used to validate the results. Analytical calculations are required for the dimensioning tool. Design optimization is carried out by a practical engineering approach, comparing different options and their effect on the total mass and estimated costs.

1.5 Framing

There are multiple types of ash hoppers in different boilers. This master's thesis will focus on one specific type of hopper, but the results can be partly applicable to other hoppers as well. The construction of the hopper is generalized, but the scale of dimensions can vary. As this thesis aims to form a general dimensioning guide for a certain type of hoppers, it will only consider structural design and detail design need to be executed manually. Hopper

structure is simplified to an adequate level with relevant assumptions in order to perform general analyses.

Special load situations like earthquake loads are left outside the scope of this thesis. Boilers are delivered to locations where earthquakes are an important aspect to be concluded in the analysis, but for these cases, the analysis has to be done separately by structural analysis.

Surrounding equipment is included in the analyses, but the design of them is not considered. Joining structures like flue gas ducts already have their own separate dimensioning guide, so they are left outside the scope of this thesis. The thesis only considers the design of the ash hopper.

2 LOADS ACTING ON THE HOPPER

The main loads acting on the hopper are the dead weight of the structures, flue gas pressure and the ash load. The size of hopper and external structures vary and therefore loads need to be considered case-by-case, but this chapter presents the principles in defining the acting loads.

2.1 The dead weight of the structures

The dead weight of the hopper can range from a few tonnes even up to 20 tonnes in the largest hoppers. The weight of insulation should also be considered. Hopper is supporting the connected components like the flue gas duct and ash conveyor. The hopper is attached from the top so the dead weight will cause mostly tensile stresses in the structure. Asymmetric weight distribution of hopper and components can also cause global moment around the hopper and concentrate the support forces on one side. The nominal loads caused by dead weight are considered with gravitational acceleration g of $9,81 \text{ m/s}^2$.

Ash conveyor is connected to the bottom of the hopper by a flange connection, so the hopper supports its weight. As a safe general assumption, the conveyor's total dead weight is assumed to be supported by the hopper. The size and mass of the ash conveyor vary based on the overall dimensions of the hopper but typically range from few tonnes up to 10 tonnes.

The flue gas duct has separate supports, but the weight is partly supported by the ash hopper. Once the flue gas duct is attached to the hopper, the duct hanger plates support both the hopper and the flue gas duct. There are bellows in the flue gas duct to account for thermal expansion and the bellows do not transmit dead load, however, bellow causes a reaction force. The dead weight of the flue gas duct is considered case-by-case.

2.2 Ash load

The function of ash hoppers is to collect and guide the ash particles to the conveyor for transportation into permanent storage. Normally the ash is not accumulating in the hopper, but the ash level can rise in the hopper if there is a blockage, or the conveyor is malfunction-

ing. The stored and flowing solid particles within the hopper then cause different load components in the walls. The definition of silo and hopper loads in different standards are based on the classic theory of silo pressures by H. A. Janssen. Load components subjected to the hopper walls from the ash load are the normal pressure p_{nf} and friction traction p_{ff} (figure 4).

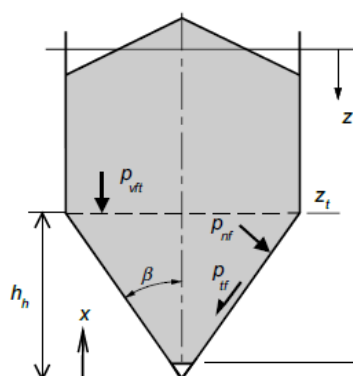


Figure 4. Ash load components of a hopper (SFS-EN 1991-1-4 2007, p. 67).

The theory and calculation of silo load components is relatively complex, and therefore it is not relevant to present it in detail in this thesis. The load components acting on the hopper walls are calculated according to SFS-EN 1991-1-4.

The hopper angle is a key variable of hopper load components as it defines the distribution between normal pressure and friction traction. Various particulate solid properties also affect the loads. The fly ash density varies depending on the fuel and boiler type, but typically, the ash density ρ is 700-1000 kg/m³. Table 1 presents the general fly ash properties needed in the calculation of hopper loads.

Table 1. Particulate solid properties (SFS-EN 1991-1-4 2007, p. 99).

Type of particulate solid ^{d, e}	Unit weight ^b		Angle of repose ϕ_r	Angle of internal friction ϕ_i		Lateral pressure ratio K		Wall friction coefficient ^c μ ($\mu = \tan \phi_w$)			Patch load solid reference factor C_{op}	
	γ_ℓ	γ_u		ϕ_{im}	a_ϕ	K_m	a_K	Wall type D1	Wall type D2	Wall type D3		a_μ
	Lower	Upper		Mean	Factor	Mean	Factor	Mean	Mean	Mean	Factor	
	kN/m ³	kN/m ³	degrees	degrees								
Default material ^a	6,0	22,0	40	35	1,3	0,50	1,5	0,32	0,39	0,50	1,40	1,0
Flyash	8,0	15,0	41	35	1,16	0,46	1,20	0,51	0,62	0,72	1,07	0,5

Simple hydrostatic pressure load is calculated for comparison of the silo loads. The hydrostatic pressure load of ash is defined by the equation where z is a coordinate along the height of the hopper (Valtanen 2019, p. 185):

$$p_{ash} = \rho g z \quad (1)$$

Calculation of hopper loads using different methods was done for comparison. Figure 5 presents the calculated load components in an example hopper with a hopper height of 1500 mm and hopper angles of 40° .

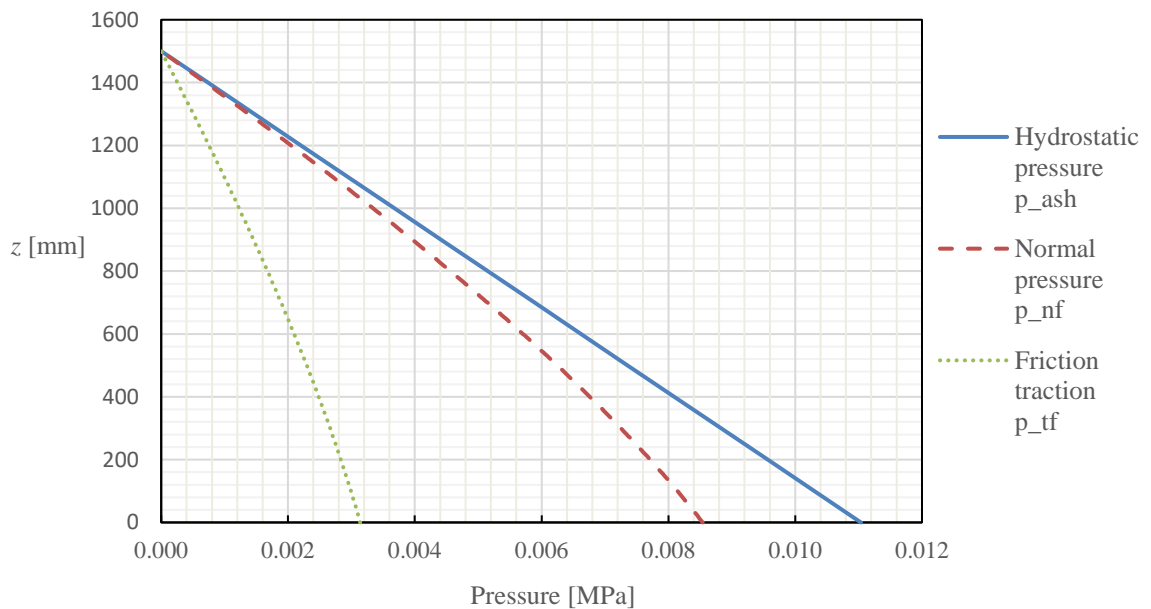


Figure 5. Load components of ash along the height of hopper according to SFS-EN 1991-1-4 and by hydrostatic pressure load.

2.3 Flue gas pressure

The acting flue gas pressure p_{fg} is boiler-specific, and it can be either negative or positive. Both the maximum and minimum values are considered in the analysis. In NFPA (National Fire Protection Association) compliant projects the design pressure is $\pm 8,7$ kPa (NFPA 85 2019, p. 170).

2.4 Temperatures

The acting flue gas temperature vary based on the boiler type, ash hopper location within the boiler and overall configuration of the hoppers. The design temperature is determined based on the process design parameters and typically can range from 200°C to 550°C. The hot flue gas flows through and the whole hopper is thermally insulated from the outside. Based on previous analyses, the temperatures between components are assumed to be relatively even, and therefore the stresses due to thermal elongation to be minor. The thermal elongation in joining structures like flue gas ducts is allowed with bellows.

2.5 Partial safety factors and load combinations

Load combinations should consider all the most unfavorable design situations that can occur. Limit states are used to distinguish design situations for the analyses. Eurocode divides the limit states into 2 categories: SLS (serviceability limit states) and ULS (ultimate limit states) (SFS-EN 1990 2002, p. 27). Structural strength is verified by ULS and deformations are checked by SLS. Limit state design is presented in detail in chapter 3.2.

Load partial safety factors consider the uncertainties related to loads and load effects. SFS-EN 1990 recommends partial safety factors for actions in different ultimate limit state analyses. For serviceability limit state analyses, all partial factors should be taken as 1.0 (SFS-EN 1990 2002, pp. 47, 54). The general form of a combination of actions is expressed as (SFS-EN 1990 2002, p. 44):

$$\sum_{j>l} \xi_j \gamma_{G,j} G_{k,j} + \gamma_P P + \gamma_{Q,1} Q_{k,1} + \sum_{i>l} \gamma_{Q,1} \psi_{0,i} Q_{k,i} \quad (2)$$

where

- ξ_j is a reduction factor for unfavorable permanent actions
- $\gamma_{G,j}$ is a partial factor for permanent actions
- $G_{k,j}$ is the design value of permanent action
- γ_P is a partial factor for prestressing actions
- P is the design value of prestressing action
- $\gamma_{Q,1}$ is a partial factor for variable actions
- $Q_{k,1}$ is the design value of variable action
- $\psi_{0,i}$ is the reduction factor for accompanying variable actions

Recommended partial safety factor for unfavorable permanent actions $\gamma_{G,j}$ is 1.35 and for leading and accompanying variable actions $\gamma_{Q,i}$ is 1.50. When both permanent and variable actions are analyzed in a load combination, the reduction factor for permanent actions can be used $\xi_j = 0,85$, so the total partial factor for permanent actions reduces to $0,85 \cdot 1,35 \approx 1,15$. (SFS-EN 1990 2002, p. 52.) Dead weight is considered as permanent action and the ash load is the main variable action and flue gas pressure is the accompanying variable action. The partial factor for accompanying variable actions can be lowered by factor $\psi_{0,i}$ as the interaction of maximum flue gas pressure and maximum ash load is an unlikely situation. Factor of $\psi_{0,i} = 0,7$ is used.

The following loads are acting on the hopper:

- A.** Dead weight of the structures
- B.** Ash load
- C.** Positive flue gas pressure
- D.** Negative flue gas pressure

Table 2 presents the load combinations used in the analysis with the corresponding partial safety factors. Load case with only dead weight is not considered as it is covered by the other cases. Load case 1 is determining load case based on the stresses and deformations and load case 2 can be determining case considering the stability.

Table 2. Load cases and partial factors for limit states.

Load case	ULS	SLS
1. Ash load + positive pressure	$1.15A + 1.5B + 1.05C$	$A + B + C$
2. Empty hopper + negative pressure	$1.15A + 1.05D$	$A + D$

3 DESIGN CRITERIA OF AN ASH HOPPER

Ash hopper is a welded plate structure. It consists of rectangular straight plates and beam profiles. The hopper wall plates form the main structure, and they are stiffened with additional plates or beams. The inside tension rods stiffen the walls generally and carry loads from walls mostly as axial forces. All parts in the hopper are connected by welds and therefore welding is a major part of the design and assembly. This chapter introduces the design criteria and presents the most relevant theory needed in the analysis of the structure. The design criteria are set by considering relevant standards, different load conditions and possible failure modes in the structural members of the hopper.

3.1 Standards guiding the design of an ash hopper

Different standards provide guidelines for the design of a hopper. Ash hopper however is a special component so there is not a specific standard that would set explicit requirements for it. European design standards are applied to cover the different conditions and components of the hopper. In addition to standards, the equations and practices from the strength of materials are utilized with appropriate material properties. The guidelines for design criteria, load definitions and material properties can be mostly obtained from standards:

- EN 1990 *Basis of structural design.*
- EN 1991-1-4 *Actions on structures. Silos and tanks.*
- EN 1993-1-1 *Design of steel structures. General rules and rules for buildings*
- EN 1993-1-5 *Design of steel structures. Plated structural elements.*
- EN 1993-1-7 *Design of steel structures. Plated structures subject to out-of-plane loading.*
- EN 1993-1-8 *Design of steel structures. Design of joints.*
- EN 1993-4-1 *Design of steel structures. Silos.*
- EN 10028-2 *Flat products made of steels for pressure purposes. Non-alloy and alloy steels with specified elevated temperature properties.*
- EN 13084-7 *Free-standing chimneys. Product specifications of cylindrical steel fabrications for use in single wall steel chimneys and steel liners.*

Plates form the main structure of the hopper and rules for general plate structures can be applied. Ash load and pressures cause loads mainly along the normal of the plate walls, referred as out-of-plane loading. SFS-EN 1993-1-7 presents design criteria and applicable analysis methods for stiffened and unstiffened plate sections subjected to out-of-plane loading. Based on the standard, analysis can be carried out using the following methods but with certain limitations:

- a) Using standard formulas with appropriate boundary conditions
- b) Global numerical analysis
- c) Simplified methods
 - dividing plates into individual segments
 - considering stiffened plate as a grill

(SFS-EN 1993-1-7 2007, pp. 10-13.)

The global out-of-plane loading also causes in-plane compressive and tensile forces in structural members such as stiffeners and in the wall panels locally. SFS-EN 1993-1-5 presents rules for plated elements subjected to in-plane loads. Standard provides additional details and methods for considering the effective width and buckling of plates due to compressive stress.

Ash hopper can be partly considered as a silo structure as SFS-EN 1993-4-1 includes rules for rectangular and pyramidal silo- and hopper structures. Major differences are the top attachment of the hopper, flue gas duct located on the side and special conditions like high temperatures. This standard can be mainly used as a reference guideline for determining the recommended analysis and design criteria. Modeling and analysis of rectangular silo structure should follow the rules from SFS-EN 1993-1-7. Additionally, the following conditions should be met when applicable:

- All stiffeners, large openings and attachments should be included
- The design should satisfy the assumed boundary conditions
- The joints should satisfy the modeling assumptions for strength and stiffness
- Each panel of the wall can be treated as an individual plate if flexural stiffnesses and forces and moments of adjacent panels are included

(SFS-EN 1993-4-1 2007, p. 31.)

Standard categorizes silo structures into consequence classes based on capacity and design situations and different analysis methods are required for each class. Figure 6 presents the determination of the consequence class for silos. Situations are not directly comparable to ash hoppers, but definitions are used as a reference.

Consequence Class	Design situations
Consequence Class 3	Ground supported silos or silos supported on a complete skirt extending to the ground with capacity in excess of W_{3a} tonnes Discretely supported silos with capacity in excess of W_{3b} tonnes Silos with capacity in excess of W_{3c} tonnes in which any of the following design situations occur: a) eccentric discharge b) local patch loading c) unsymmetrical filling
Consequence Class 2	All silos covered by this Standard and not placed in another class
Consequence Class 1	Silos with capacity between W_{1a} tonnes† and W_{1b} tonnes
† Silos with capacity less than W_{1a} tonnes are not covered by this standard.	

The recommended values for class boundaries are as follows:

Class boundary	Recommended value (tonnes)
W_{3a}	5000
W_{3b}	1000
W_{3c}	200
W_{1b}	100
W_{1a}	10

Figure 6. Determination of consequence class for silos (SFS-EN 1993-4-1 2007, p. 21).

Most ash hoppers can be then considered as a consequence class 1 since their capacity is less than 100 tonnes. Based on the standard, the internal forces in the plate segments may then be determined using three different methods:

- static equilibrium for membrane forces and beam theory for bending
- an analysis based on linear plate bending and stretching theory
- an analysis based on nonlinear plate bending and stretching theory

(SFS-EN 1993-4-1 2007, p. 32.)

For consequence class 1 and symmetrically loaded plates of consequence class 2, the simplified method (a) may be used. For consequence class 3 and asymmetrically loaded plates of consequence class 2, the method (b) or (c) may be used. Use of a higher consequence class is always possible (SFS-EN 1993-4-1 2007, p. 32). Required analysis criteria for classes 1 and 2 can be fulfilled either by analytical calculations or by numerical methods like linear FEA. The analytical approach requires careful simplifications to the structure but with a correctly constructed FE-model, necessary phenomena are considered therefore making it a more accurate method. Based on the standard, non-linear methods are not required for a

basic global analysis of silos with the corresponding scale, but ash hopper is not explicitly considered a silo. Applicable methods should be considered case-by-case and comparative tests conducted to ensure proper representation of the structural behavior.

As a summary of recommended analysis methods, simple analytical calculation methods can be used if the methods are verified appropriately. The structure can also be divided into individual sections for analysis if the details and connections between sections are verified. Global numerical analysis is recommended for all situations.

The definition of the silo- and hopper loads are obtained from SFS-EN 1991-1-4. It presents the calculation of load components caused by filling and discharging solid ash particles in the hopper. Other loads and properties such as flue gas pressure and fly ash density are product-specific and obtained from Valmet. Recommended partial safety factors for actions and strength are obtained from relevant Eurocodes.

EN-materials that have been previously utilized are only considered in this thesis. Material selection includes structural- and pressure-grade carbon steels and alloyed steels. Material properties of utilized steels can be obtained from various standards. As the temperatures of the hopper may exceed 550°C, material properties at elevated temperatures are needed along with specific properties like creep strength. SFS-EN 10028-2 presents specific elevated temperature properties for pressure grade steels and alloyed steels. Additionally, elevated temperature properties of structural steels can be obtained from SFS-EN 13084-7, as referenced by silo design standard (SFS-EN 1993-4-1 2007, p. 25).

SFS-EN 1990 is the general Eurocode, and it presents basic rules and principles for structural analysis. General design criteria and definitions of limit states are introduced. Standard also presents recommended partial safety factors for different types of loads that can be used if not otherwise presented in more detailed standards. SFS-EN 1993-1-1 includes rules and calculation procedures for the stability of structural members. Design rules and strength calculation of welded connections are provided in SFS-EN 1993-1-8. The structural fire design standard SFS-EN 1993-1-2 is partly applicable in considering the effect of high temperatures.

3.2 Limit state design

Modern design instructions like Eurocodes utilize limit state design. Limit states are certain design criteria for the structure that it must fulfill. Limit states are applicable for all structural members, but the limiting criteria might vary for each component and structure. Limit state conditions are analyzed with the addition of the partial factor method by applying limit state-specific safety factors for each load component and safety factors on material strength properties and other uncertainties (SFS-EN 1990 2002, p. 38). Limit states relevant for ash hoppers are introduced in chapters 3.2.1. and 3.2.2.

3.2.1 Serviceability limit states

Serviceability limit states correspond to the usability and functionality of the structure. It also includes aspects like appearance and the comfort of people using the machine or structure. Serviceability limit states are further divided into reversible and irreversible states based on the effect. (SFS-EN 1990 2002, pp. 28-29.) Exceeding the serviceability limit state does not directly cause the collapse of the structure, but it can affect the usability and damage the component in such a way that overall usability is lowered.

In the case of ash hopper, the most valid serviceability limit states to be considered are:

- Deflection of wall panels locally or globally
- Local deformation
- Vibrations or oscillation

SFS-EN 1993-4-1 recommends limiting values for deflection in rectangular silo walls. Recommended values are used for reference and specific limiting values can be agreed based on the case. Recommended global maximum out-of-plane deflection δ_{max} should be taken as the minimum of (Mod. SFS-EN 1993-4-1 2007, p. 102):

$$\delta_{max} = \min (k_1 H, k_2 t) \quad (3)$$

where k_1 and k_2 are specific factors and H is the overall height of the structure and t is the thinnest wall thickness. Recommended values for factors are $k_1 = 0.02$ and $k_2 = 10$. (SFS-EN 1993-4-1 2007, p. 102.) Maximum out-of-plane deflection in a single plate segment relative to its edges should be limited to:

$$\delta_{max} < k_3 a \quad (4)$$

where k_3 is a specific factor and a is the shorter side of a rectangular plate. Recommended value for factor $k_3 = 0.05$. (SFS-EN 1993-4-1 2007, p. 103.)

Local deformations can occur in different structural members. Small local deformations do not cause disturbance in the normal operation of a hopper. Vibrations or oscillations can occur from fluctuating pressures or by natural frequencies. Vibrations can cause abnormal behavior and noises in the structure or even damage. In the case of ash hoppers, vibrations are not considered to be a major risk due to the nature of loads and adequate stiffening.

In the case of ash hopper, serviceability criteria are not the determinative aspect. Hopper is a statically working structure that has no special requirements for functionality. Deflections or deformations do not easily affect the normal operation and risks of vibrations or oscillation are low. The design is driven by structural strength requirements.

3.2.2 Ultimate limit states

Ultimate limit states correspond to states that concerns the safety of the people and the structure. Exceeding the ultimate limit state will cause the collapse of the structure or part of the structure. (SFS-EN 1990 2002, p. 28.) Ultimate limit states are divided into 4 categories:

- EQU: Loss of static equilibrium
- STR: Structural failure, internal failure, or excessive deformation
- GEO: Geotechnical failure or excessive deformation in the ground of foundation
- FAT: Fatigue failure

(SFS-EN 1990 2002, p. 42.)

Structural failure and fatigue failure are relevant when concerning the ash hopper. Ultimate limit states can be further divided by failure modes for the examination of different structural members under load conditions. The most important failure modes of an ash hopper corresponding to ultimate limit states include:

- Plasticity or plastic mechanism
- Fracture or failure of a member or a weld joint
- Loss of stability

Structural failure can also occur due to mechanical or thermal fatigue, but it is not considered a major risk in an ash hopper. The overall temperature distribution or the loads do not vary greatly during the boiler operation and normally there are no sudden temperature changes or impact loads. The dimensioning is based on static loads.

Detailed design criteria leading to mentioned failure modes are presented in the following chapters. Specific partial safety factors for different load combinations and materials are considered in ultimate limit state analyses. The load combinations and the corresponding partial safety factors are presented in chapter 2.5. Adequate structural strength is verified by ultimate limit states.

In addition to load partial factors, partial resistance factors are recommended for certain details and failure modes. Table 3 presents the relevant resistance factors and corresponding recommended values for silo structures. Additional resistance is recommended against loss of stability, wall rupture, fatigue and failure of connections. (SFS-EN 1993-4-1 2007, p. 23.)

Table 3. Partial resistance factors for silo structures (SFS-EN 1993-4-1 2007, p. 23).

Resistance to failure mode	Relevant γ	Recommended value
Resistance of welded or bolted shell wall to plastic limit state	γ_{M0}	1.00
Resistance of shell wall to stability	γ_{M1}	1.10
Resistance of welded or bolted shell wall to rupture	γ_{M2}	1.25
Resistance of shell wall to cyclic plasticity	γ_{M4}	1.00
Resistance of connections	γ_{M5}	1.25
Resistance of shell wall to fatigue	γ_{M6}	1.10

3.3 Plates

The hopper walls consist of stiffened plates. The whole walls can be considered as grill formed by the stiffener profiles or alternatively consider the single plate segments surrounded by the stiffeners individually. The longer side of individual plate segment b is defined by the span of vertical stiffeners and the smaller side of a plate a is defined by the span of horizontal stiffeners (figure 7). For the most efficient solution, both dimensions should be maximized with an optimal b/a ratio, without exceeding the design strengths.

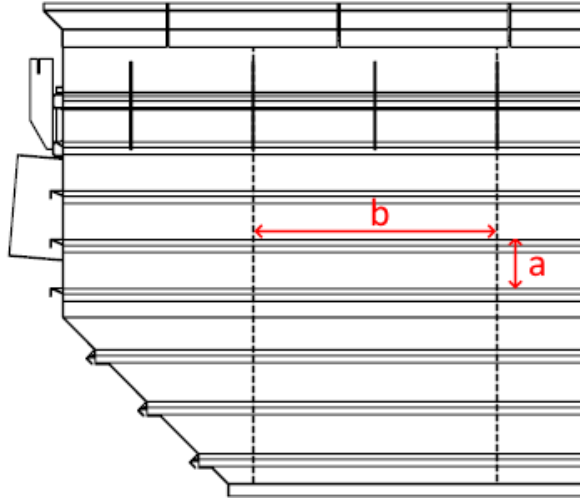


Figure 7. Plate segment defined by the stiffeners in a hopper wall.

Plate is a structural member with a small thickness compared to other dimensions. Various theories have been developed to assess the structural behavior of plates. The most commonly used theory is the classic plate theory, also known as the Kirchhoff plate theory. The classic plate theory has an analogy to beam theory, and additional assumptions are made to simplify the 3-dimensional plate case into 2-dimensional. The theory assumes that normals of the midsurface remain normal to deformed midsurface and there is no transverse strain through the thickness of the plate. The theory is based on linear elasticity and small deflections. (Bhaskar & Varadan 2021, pp. 12-15.) Figure 8 presents a general plate subjected to out-of-plane loading and the corresponding governing equation for the deflection w is expressed as follows (SFS-EN 1993-1-7 2007, p. 19):

$$\frac{\partial^4 w}{\partial x^4} + 2 \frac{\partial^4 w}{\partial x^2 \partial y^2} + \frac{\partial^4 w}{\partial y^4} = \frac{p(x, y)}{D} \quad (5)$$

Where flexural rigidity of plate D is defined as (SFS-EN 1993-1-7 2007, p. 19):

$$D = \frac{Et^3}{12(1 - \nu^2)} \quad (6)$$

where E is Young's modulus
 ν is Poisson's ratio

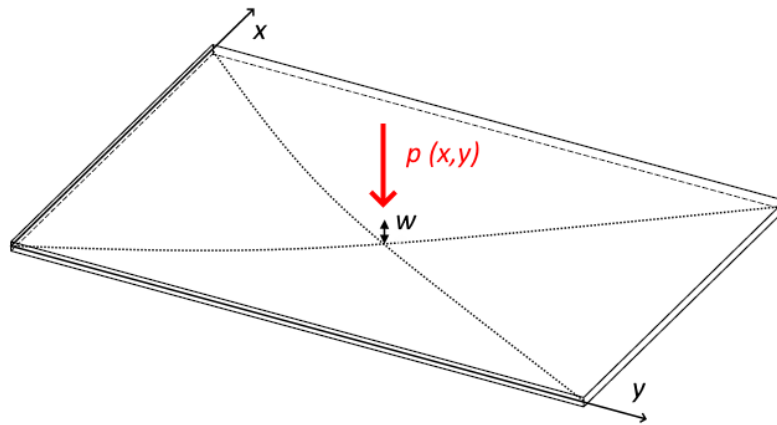


Figure 8. Deflection of a plate subjected to out-of-plane loading.

The exact solution of the plate problem can be found in limited cases but numerical solutions for various plates and conditions are tabled by different sources. SFS-EN 1993-1-7 presents tabled values of coefficients for easy calculation of transversely loaded rectangular plates. Values are pre-calculated for different boundary conditions, load types and dimension ratios of rectangular plates. The calculated coefficients take into account Poisson's ratio ν of 0.3. Tabled coefficients for plates under uniformly distributed loading with pinned and fixed boundary conditions based on small deflection theory are presented in tables 4 and 5.

Table 4. Coefficients for rectangular plate subjected to uniformly distributed loading with pinned boundary conditions (SFS-EN 1993-1-7 2007, p. 22).

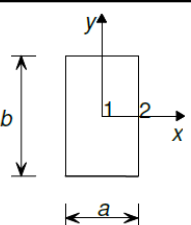
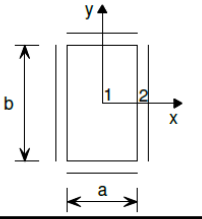
		Loading: Uniformly distributed loading	
		Boundary conditions: All edges are rigidly supported and rotationally free	
b/a	k_{w1}	$k_{\sigma_{bx1}}$	$k_{\sigma_{by1}}$
1,0	0,04434	0,286	0,286
1,5	0,08438	0,486	0,299
2,0	0,11070	0,609	0,278
3,0	0,13420	0,712	0,244

Table 5. Coefficients for rectangular plate subjected to uniformly distributed loading with fixed boundary conditions (SFS-EN 1993-1-7 2007, p. 22).

		Loading: Uniformly distributed loading		
		Boundary conditions: All edges are rigidly supported and rotationally fixed.		
b/a	k_w	$k_{\sigma_{bx1}}$	$k_{\sigma_{by1}}$	$k_{\sigma_{bx2}}$
1,0	0,01375	0,1360	0,1360	-0,308
1,5	0,02393	0,2180	0,1210	-0,454
2,0	0,02763	0,2450	0,0945	-0,498
3,0	0,02870	0,2480	0,0754	-0,505

Small deflection theory does not account for membrane stresses in the plate, so coefficients for bending stresses and coefficient for deflection are only presented. Table variables are the coefficients for bending stresses around x-axis $k_{\sigma_{bx}}$ and y-axis $k_{\sigma_{by}}$ and a coefficient for deflection k_w . Denotation after the subscripts refer to the corresponding location in the plate. For uniformly distributed loading the bending stress around x-axis $\sigma_{bx,Ed}$ can be calculated as (SFS-EN 1993-1-7 2007, p. 21):

$$\sigma_{bx,Ed} = k_{\sigma_{bx}} \frac{q_{Ed} a^2}{t^2} \quad (7)$$

where q_{Ed} is the design value of uniformly distributed loading

Consequently, the bending stress around y-axis $\sigma_{by,Ed}$ can be calculated as (SFS-EN 1993-1-7 2007, p. 22):

$$\sigma_{by,Ed} = k_{\sigma_{by}} \frac{q_{Ed} a^2}{t^2} \quad (8)$$

The stress components can then be combined into equivalent von Mises stress $\sigma_{eq,Ed}$ with the equation, assuming no shear stresses occurs in the plate (SFS-EN 1993-1-7 2007, p. 22):

$$\sigma_{eq,Ed} = \sqrt{\sigma_{bx,Ed}^2 + \sigma_{by,Ed}^2 - \sigma_{bx,Ed} \cdot \sigma_{by,Ed}} \quad (9)$$

The deflection of a plate w can be calculated with equation (SFS-EN 1993-1-7 2007, p. 21):

$$w = k_w \frac{q_{Ed} a^4}{Et^3} \quad (10)$$

Tables do not present coefficient for bending stress around y-axis $\sigma_{by,Ed}$ at the edge of the longer side, but due to bending around the x-axis and constraints, the y-stress component is also formed. Von Mises stress at the longer edge is calculated so the maximum stresses are easily comparable with FEA. The bending stress around y-axis $\sigma_{by,Ed}$ at the longer side of the plate is approximated using Poisson's theory:

$$\sigma_{by,Ed} = \nu \sigma_{bx,Ed} \quad (11)$$

Calculation with the coefficients is fast and simple but there are limitations. The coefficients are tabled with a minimum of 0.5 intervals so the intermediate values should be interpolated for better accuracy. The small deflection theory also has limitations, as the calculated deflection w should be below $t/2$ for reasonable accuracy with the theory (Niemi & Kemppe 1993, p. 154). Selection of correct boundary conditions is the most important factor defining the accuracy of results. In a continuous stiffened plate, the edges defined by stiffeners can be considered relatively rigid and the effect of joining plates can be ignored due to symmetry at the plate edges. Appropriate boundary conditions should still be verified by testing.

As the plate deflection increases, the small deflection theory overestimates the plate stresses and gives conservative results. When the deflection in a plate increases, membrane stresses occur and start to carry the loading. (Niemi & Kemppe 1993, p. 154.) Large deflection theory considers the membrane stresses and therefore it can give higher capacity. SFS-EN 1993-1-7 also presents the tabled coefficients for calculation by large deflection theory but the small deflection theory is considered to be adequate for ash hopper plate segments, so the more complicated calculation by large deflection theory is not presented.

3.4 Stiffeners

Stiffeners in a plate are used to increase buckling resistance or limit the global stresses and deflection. When a plate is subjected to out-of-plane loading, the main purpose of stiffeners

is to help carry the plate bending moments and then limit global deflection and overall stress. Plate bending moment is determining in the direction of shorter stiffeners, so it is more efficient to control stresses by limiting the plate dimension a using stiffeners. The stiffeners along the long side resist the total deflection of the plate and the stress of stiffener itself can be determining in this direction. For compressive in-plane loads, the stiffeners are used to increase buckling capacity by dividing the plate into smaller sections. Buckling capacity can mainly be increased by stiffeners along the long side of the plate. Long stiffeners divide the plate into narrow sections which are more resistant to buckling. (Niemi 2003, p. 19.)

When stiffeners are welded to the hopper walls with adequate strength welds, the stiffener and width of the plate can be considered as a uniform profile. The full width of the plate wall between stiffeners cannot be utilized due to shear lag. In a thin and wide flange connected to a web, the shear deformations are not uniform across the width of the flange, and stresses are distributed closer to the web. This means that the edges of wide plates are not stressed and cannot be considered fully effective. (Niemi 2003, p. 38.) Eurocode considers shear lag by reducing the plate width into effective width. In a rectangular silo wall, the effective width of plate flange B_{eff} on each side of stiffener should be taken as (SFS-EN 1993-4-1/AC 2009, p. 2):

$$B_{eff} = n_{ew}t \quad (12)$$

where recommended value for effective width factor n_{ew} is 15ε and coefficient ε is defined by the equation where f_y is the yield strength:

$$\varepsilon = \sqrt{235/f_y} \quad (13)$$

The total effective flange width is then $2B_{eff}$. Figure 9 presents the definition of effective width in a plate wall horizontally stiffened by L-profiles. Vertical stiffeners are considered with the same principle.

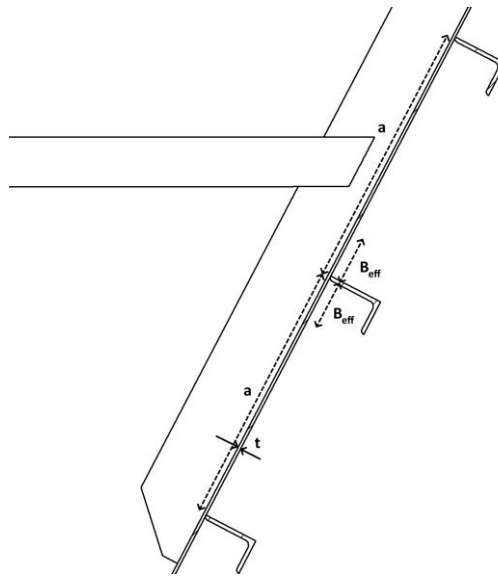


Figure 9. Determination of effective width of wall plate stiffened by L-profiles.

The effective width of the wall plate connected to the stiffener may also be determined by SFS-EN 1993-1-5. The method is suitable for general structures and it is used for comparison and verification of suitable method for the case. For the calculation of effective width, the effective length of the stiffener in a plate segment is first obtained as defined in figure 10. Length of stiffener L_{stiff} is reduced to effective length L_e based on the location and boundary conditions of the stiffener.

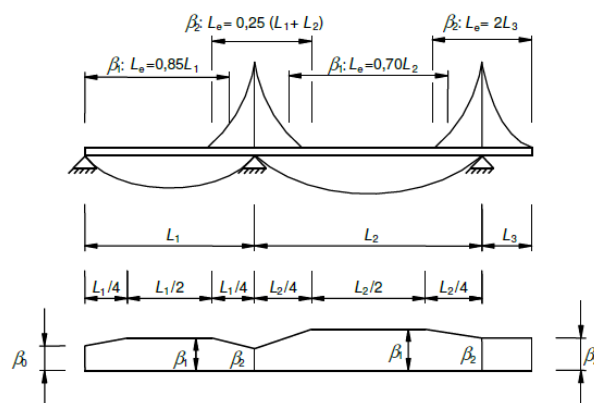
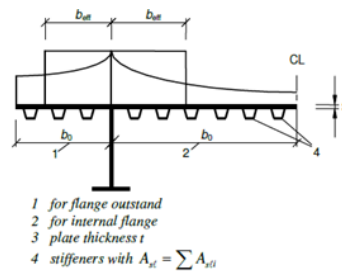


Figure 10. Determination of effective length (SFS-EN 1993-1-5 2006, p. 8).

The final effective width factor β is calculated by selecting the correct equation for factor κ based on the sign of bending moment from figure 11 (SFS-EN 1993-1-5 2006, p. 9).



κ	Verification	β - value
$\kappa \leq 0,02$		$\beta = 1,0$
$0,02 < \kappa \leq 0,70$	sagging bending	$\beta = \beta_1 = \frac{1}{1 + 6,4 \kappa^2}$
	hogging bending	$\beta = \beta_2 = \frac{1}{1 + 6,0 \left(\kappa - \frac{1}{2500 \kappa} \right) + 1,6 \kappa^2}$
$> 0,70$	sagging bending	$\beta = \beta_1 = \frac{1}{5,9 \kappa}$
	hogging bending	$\beta = \beta_2 = \frac{1}{8,6 \kappa}$
all κ	end support	$\beta_0 = (0,55 + 0,025 / \kappa) \beta_1$, but $\beta_0 < \beta_1$
all κ	Cantilever	$\beta = \beta_2$ at support and at the end
$\kappa = a_0 b_0 / L_{st}$ with $a_0 = \sqrt{1 + \frac{A_{st}}{b_0 t}}$ in which A_{st} is the area of all longitudinal stiffeners within the width b_0 and other symbols are as defined in Figure 3.1 and Figure 3.2.		

Figure 11. Determination of effective width (SFS-EN 1993-1-5 2006, p. 9).

The effective width of a flange on each side of stiffener B_{eff} is then calculated by equation, where b_0 is half of the stiffener span in the corresponding direction (SFS-EN 1993-1-5 2006, p. 9):

$$B_{eff} = \beta b_0 \quad (14)$$

Various profiles are used as stiffeners. Ready-made profiles are favored since they are cheap and available. The inside vertical stiffeners are always flat bars so the tension rods can be connected to them easily, but the horizontal stiffener profiles are chosen case-by-case. Cross-section properties of combination profiles are obtained by combining the cross-sectional properties of the stiffener profile and the effective width of the plate wall. The effective width changes as other dimensions change, so it must be calculated individually for each case and then calculate the cross-section properties. Figure 12 presents the cross-sections of various stiffener profiles and table 6 presents the corresponding cross-section properties. Properties are obtained by Solidworks 2020 CAD-software.

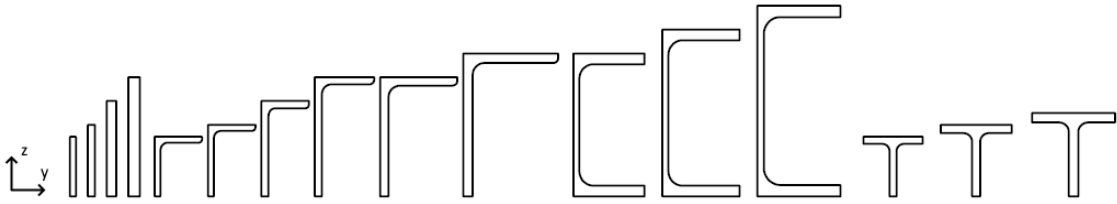


Figure 12. Cross-sections of various stiffener profiles.

Table 6. Cross-section properties of stiffener profiles (computed with Solidworks 2020).

Stiffener profile	Cross-sectional area A [mm ²]	Distance of neutral axis from bottom z_0 [mm]	Second moment of area I_y [mm ⁴]
Flat 50x5	250	25	52083,3
Flat 60x6	360	30	108000
Flat 80x8	640	40	341333,3
Flat 100x10	1000	50	833333,3
L 50x40x5	430,8	34,4	132643,2
L 60x40x5	480,8	40,3	200365,7
L 80x40x6	692,2	51,2	483498,2
L 100x50x6	874,3	64,7	967563,8
L 100x65x7	1124	67,4	1306751,2
L 120x80x8	1554	81,3	2644155,5
U 120	1651,8	60	3920744,9
U 140	1841,8	70	5994616,9
U 160	2189,6	80	9208447,1
T 50x6	579,4	35,4	132092,6
T 60x7	812	42,7	267550,2
T 70x8	1083,5	49,8	487183,9

The combined area of stiffener and effective width of plate A_{prof} is calculated by summing the areas of components together (SFS-EN 1993-1-3 2006, p. 121):

$$A_{prof} = \sum_{i=1}^n dA_i \quad (15)$$

The center of the area in y- and z-direction also defines the position of the neutral axis in both directions. The center of area in the y-axis and neutral axis position around z-axis y_0 is calculated as (Salmi & Pajunen 2018, p. 410):

$$y_0 = \frac{\int \int y dA}{A} = \frac{\sum_{i=1}^n A_i y_i}{\sum_{i=1}^n A_i} \quad (16)$$

Consequently, the center of the area in the z-axis and neutral axis position around y-axis z_0 is calculated as (Salmi & Pajunen 2018, p. 410):

$$z_0 = \frac{\int \int z dA}{A} = \frac{\sum_{i=1}^n A_i z_i}{\sum_{i=1}^n A_i} \quad (17)$$

The second moment of the area around the y-axis of the combination profile is calculated as (Salmi & Pajunen 2018, p. 410):

$$I_y = \int \int z^2 dA = \sum_{i=1}^n I_{y,i} + A_i d_{z,i}^2 \quad (18)$$

where $I_{y,i}$ is the second moment of area of individual component around y-axis
 $d_{z,i}$ the distance between components neutral axis and combination profile's
 neutral axis in z-direction

The second moment of the area around the z-axis of the combination profile is calculated as (Salmi & Pajunen 2018, p. 410):

$$I_z = \int \int y^2 dA = \sum_{i=1}^n I_{z,i} + A_i d_{y,i}^2 \quad (19)$$

where $I_{z,i}$ is the second moment of area of individual component around z-axis
 $d_{y,i}$ the distance between components neutral axis and combination profile's
 neutral axis in y-direction

In unsymmetrical L- and U-profiles the center of the area or the torsion center is not located along the center of the flange line (figure 13). The resultant of the pressure load is subjected to the flange line and therefore the load is eccentric regarding the center of the area and torsion center. This causes additional stress by secondary distortion and torsion in the profile.

However, the effect is considered small and neglectable in analytical calculations, but the effect is considered in FEA when utilizing shell or solid elements.

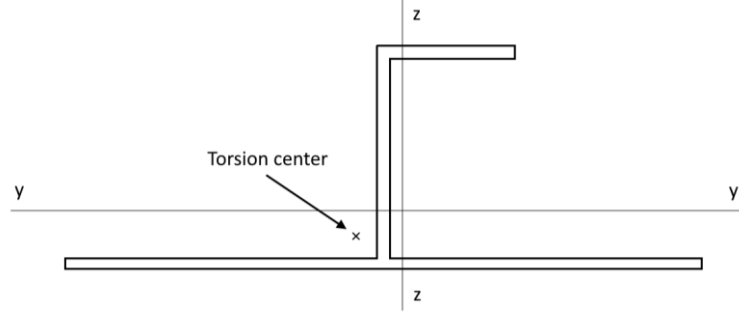


Figure 13. Principle locations of the center of area and torsion center in plate wall stiffened by L-profile.

The combination profile may be analyzed by considering it as a beam. A single stiffener carries the pressure load of half a plate segment on each side of the stiffener. The pressure exerted on the plate segment may be expressed as a line load q to the combination profile:

$$q = (p_{fg} + p_{ash}) a \quad (20)$$

The stiffener is a continuous profile along the plate wall, so the length of the stiffener in a plate segment may be considered as a beam rigidly supported by its edges. The maximum bending moment M_{max} of a rigidly supported beam is at support (Valtanen 2019, p. 323):

$$M_{max} = \frac{-qb^2}{12} \quad (21)$$

The bending stress of stiffer σ_{stiff} may then be calculated by a general equation for bending stress:

$$\sigma_{stiff} = \frac{-(p_{fg} + p_{ash}) ab^2}{12W} \quad (22)$$

and section modulus W is defined by an equation where c is the maximum distance from the neutral axis:

$$W = \frac{I_y}{c} \quad (23)$$

The outside horizontal stiffener profiles surround the hopper walls, but stiffeners cannot be directly joined together at the corners due to the angles of hopper walls. Corner plates are used to join the flanges of stiffener profiles, so the stiffeners will work as a uniform arc around the hopper and can transfer the forces across corners to take the stress away from the wall corner joints (figure 14).

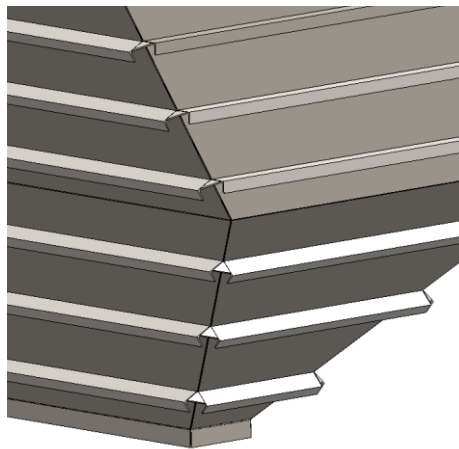


Figure 14. Corner plates between horizontal stiffeners.

Tension rods are part of the stiffening structure. Rods effectively stiffen and reduce stresses in whole plate walls by shortening the support lengths of stiffeners and therefore reducing the bending moments. Respectively it also has an effect on the stress of plate segments. Tension rods are attached to the junctions of stiffeners to support both vertical and horizontal stiffeners efficiently. The limiting criteria for tension rods are the loss of stability under negative pressure or plasticity due to tensile forces with ash load and positive pressure. SFS-EN 1993-4-1 refers to tension rods as internal ties and presents ways of assessing the internal forces. By a simple method, the force per unit length of tie q_t may be approximated by (SFS-EN 1993-4-1 2007, p. 98):

$$q_t = C_t p_v b_t \quad (24)$$

with:

$$C_t = \frac{C_s \beta_t}{k_L} \quad (25)$$

where p_v is the vertical pressure within the stored material at the tie level
 b_t is the maximum horizontal width of the tie
 C_t is the load magnification factor
 C_s is the shape factor for the tie cross-section
 k_L is the loading state factor
 β_t is the tie location factor, that depends on the position of the tie within a silo

The value for shape factor C_s for circular profiles is recommended to be 1.0 and the highest value for loading state factor k_L is during discharge and is recommended to be 4.0. For all ties of ash hopper, the location factor β should be taken as 1.0 since all tension rods are between opposite walls. (SFS-EN 1993-4-1 2007, p. 99.)

The tension rod forces can be simply estimated by dividing the wall segments into pressure areas supported by the corresponding tension rods. The pressure area for rod A_{rod} is considered as the area bounded by half the tension rod span in vertical and horizontal directions. The method does not consider the boundary conditions or stiffness of the wall, so the obtained results should be conservative as the tension rods are assumed to support the total pressure load of the walls. The axial force N_{Ed} is then calculated by multiplying the pressure area with the total pressure exerted on the area and considering the specific wall angle α_{wall} :

$$N_{Ed} = \cos(\alpha_{wall}) \cdot A_{rod} \cdot (p_{fg} + p_{ash}) \quad (26)$$

The tension rod forces are more accurately obtained by numerical methods like FEA. The use of method presented in SFS-EN 1993-4-1 should be verified since the hopper structure cannot be explicitly considered as a rectangular silo. When using more detailed numerical methods, geometrically non-linear analysis (GNA) is recommended to be performed to determine the rod axial forces N_{Ed} and bending moments M_{Ed} . GNA takes into account the second-order effects and stiffness of hopper walls. (SFS-EN 1993-4-1 2007, p. 99.)

3.5 Effect of high temperatures on materials

When a boiler is in operation, the ash hopper is constantly under high temperatures as hot flue gases flow through the hopper. The flue gas temperatures depend on the boiler type and configuration but can be up to 550 °C when passing through the hopper. High temperatures set special demands for the material and design. Temperatures affect the material's mechanical properties, most importantly the yield strength f_y and the ultimate strength f_u are reduced. High temperatures also introduce new harmful phenomena like creep, which is often a significant structural criterion in high-temperature applications (González-Velázquez 2020, p. 226). The temperatures also have an effect on other design criteria like the strength of welds and stability, and the relevant details are presented in the corresponding chapters.

3.5.1 Mechanical properties

Material selection in this thesis is limited to EN materials. Detailed material properties of EN-steels in high temperatures can be found from Eurocode standards so they can be reliably used in conjunction. Material properties are the key aspect in defining the allowable criteria for ultimate limit states. SFS-EN 10028-2 presents mechanical properties for flat products made of steels for pressure purposes. Table 7 presents the elevated temperature properties of relevant materials used in ash hoppers with plate thickness $t < 16$ mm. Standard only considers pressure-grade steels.

Table 7. Strength properties of flat products made of steels for pressure purposes (SFS-EN 10028-2 2017, p. 16).

Steel name	Number	For plate thicknesses $t < 16$ mm									
		Minimum 0.2 % proof strength $R_{p0.2}$ [MPa] at temperature °C									
		50	100	150	200	250	300	350	400	450	500
P235GH	1.0345	227	214	198	182	167	153	142	133	-	-
P265GH	1.0425	256	241	223	205	188	173	160	150	-	-
P355GH	1.0473	343	323	299	275	252	232	214	202	-	-
16Mo3	1.5415	273	264	250	233	213	194	175	159	147	141
13CrMo4-5	1.7335	294	285	269	252	234	216	200	186	175	164
10CrMo9-10	1.7380	288	266	254	248	243	236	225	212	187	185

SFS-EN 13084-7 presents product specifications of cylindrical steel fabrications for use in single-wall steel chimneys and steel liners (table 8), and silo standard recommends obtaining

the elevated material properties from this standard. Conditions of a chimney are also similar to ash hopper in terms of temperatures and flue gases flowing through. SFS-EN 13084-7 also presents properties of structural steel which are used in the ash hoppers. Values are only tabled for plate thicknesses t up to 40 mm, and therefore the strength values are lower than for the same materials presented in table 7. Comparing the strength properties from these standards with equal plate thicknesses, the properties are identical for the same materials. However, SFS-EN 10028-2 does not recommend the use of certain steels in as high temperatures compared to SFS-EN 13084-7. The strength values given in SFS-EN 13084-7 are slightly conservative as the usual plate thicknesses used in the hopper are less than 15 mm.

Table 8. Strength properties of steels at elevated temperatures (SFS-EN 13084-7 2013, p. 8).

Steel name	Number	For plate thicknesses $t < 40$ mm											
		Characteristic value of yield stress f_y [MPa] at temperature °C											
		50	100	150	200	250	300	350	400	450	500	550	600
S235JR	1.0038	235	190	175	160	140	120	-	-	-	-	-	-
S275JR	1.0044	275	215	200	185	165	145	125	104	-	-	-	-
S355JR	1.0045	355	260	245	230	210	190	-	-	-	-	-	-
P265GH	1.0425	247	232	215	197	181	166	154	145	80	-	-	-
16Mo3	1.5415	268	259	245	228	209	190	172	156	145	139	-	-
13CrMo4-5	1.7335	285	275	260	243	226	209	194	180	169	159	76	-
10CrMo9-10	1.7380	270	249	238	232	227	221	211	198	185	173	83	44

In addition to material strength, material behavior is also affected by temperatures. Young's modulus E displays the slope of the linear-elastic zone in the stress-strain curve. The nominal value of Young's modulus for steels is usually taken as 210 000 MPa, but as the temperatures are higher, the modulus is slightly reduced. SFS-EN 13084-7 presents values of Young's modulus for various steels in elevated temperatures. Table 9 presents the values for steels relevant to ash hopper design.

Table 9. Characteristic values of Young's modulus E for steels at elevated temperatures (SFS-EN 13084-7 2013, p. 9).

Steel name	Number	Characteristic values of Young's modulus E [GPa] at temperature °C							
		20	150	250	350	450	500	550	600
S235JR	1.0038	210	205	200	192				
S275JR	1.0044	210	205	200	192				
S355JR	1.0045	210	205	200	192				
P265GH	1.0425	210	205	200	192	184	180		
16Mo3	1.5415	210	205	200	192	184	180		
13CrMo4-5	1.7335	210	205	200	192	184	180		
10CrMo9-10	1.7380	210	205	200	192	184	180		

3.5.2 Creep

Creep is defined as plastic strain occurring with constant stress level in high temperatures. The plastic strain occurs at lower stress levels than the nominal yield stress at the corresponding temperature. Ultimately the plastic strains may lead to creep fracture. Roughly, the creep can be associated with temperatures above half of the absolute melting point of steel material (Kassner 2009, p. 3). Typically, creep is starting to be a dominant design criterion in steels exposed for long time to temperatures of 400 - 500°C as creep strain starts to occur and the creep stress is lower than the yield strength at the corresponding temperature. Short exposure times do not induce creep behavior.

Creep can be characterized into 3 stages (figure 15). Stage 1 is the transient creep stage. It starts with the initial deformation which corresponds to the applied stress. In the beginning, creep rate is high but then it decreases to a constant level as strain hardening increases. In the second stage, the equilibrium state between strain hardening and recovery is maintained, resulting in an even and minimum creep strain. This is the longest creep stage and therefore the most important as it is commonly used as the defining limit. In stage 3 tertiary creep, the strain rate is accelerated by precipitate coarsening, recrystallization, and the reduction of cross-section area. Ultimately the creation of grain boundary voids will lead to creep fracture if the stresses are high enough. (González-Velázquez 2020, pp. 227-228.)

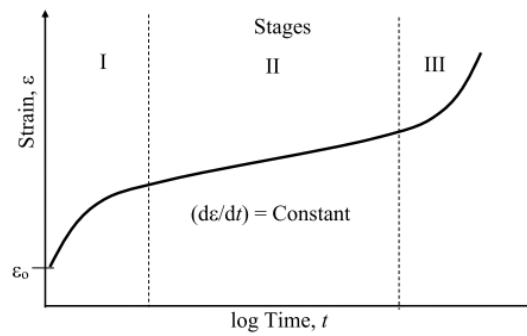


Figure 15. Stages of creep (González-Velázquez 2020, p. 228).

Eurocodes do not set specific requirements for creep in terms of analysis and design criteria, but SFS-EN 10028-2 presents creep properties of pressure-grade steels. Properties include strengths for 1% plastic creep $f_{e,1.0}$ and creep rupture strength $R_{m,c}$ for different durations. In direct engineering application it is relevant to use the readily available material data in the analysis. The creep properties for the relevant steels are presented in appendix I.

Stress levels and temperatures are not constantly high during the design life of the boiler. It is the designer's responsibility to assess and set the appropriate criteria for the applied structure based on the stress levels and estimated exposure time on the temperatures. Creep rupture strength is considered as the limiting condition for ash hoppers when flue gas temperatures are within the creep temperatures of the used materials. When temperatures are within creep temperatures, but the creep stress is higher than the corresponding yield stress, the elevated temperature yield stress should be used as the design strength $f_{y,Ed}$ (Niemi & Kemppe 1993, pp. 67-69).

Eurocodes do not directly present creep properties for structural steels that could be utilized in the calculation but SFS-EN 1993-1-2 presents rules for structural fire design for structures subjected to high temperatures. Standard presents stress-strain formulas for structural steel in different temperatures. Based on the simple models, the effective yield strength is considered to be constant until 400 °C, and at higher temperatures rapidly decrease. The model is not consistent with the material properties presented by SFS-EN 13084-7 (table 8), as the strength values are significantly reduced even below 400 °C. The structural fire design code is mainly intended for relatively short exposure times to fire and therefore the material properties are not verified to be applicable for structures exposed to high temperatures for long periods of time.

3.6 Dimensioning of welds

All parts of the hopper are joined together by welding, making it a major part of the design and assembly. Most of the welds in the hopper are fillet welds in addition to corner joints and butt welds of joining wall elements. Weld joints can be further categorized by the loading subjected to them, to enable efficient design and dimensioning. Joints can be divided into 4 categories:

- Load-bearing joints
- Fixing joints
- Binding joints
- Non-load-carrying accessory joints

(Niemi & Kemppe 1993, pp. 16-20.)

Load bearing welds join adjacent components in series, making the weld a critical component. Loading can be primary tension, compression, shear, or bending. They are often designed as equal strength to base material to provide maximum strength and deformability. Fixing welds join adjacent components in parallel to make sure components work as one part. The main loading is the shear force between joining components. (Niemi & Kemppe 1993, pp. 16-17.) Considered weld joints of the ash hopper only include load-bearing joints and fixing joints. Figure 16 presents the characterization of weld joints and joint types of a general ash hopper.

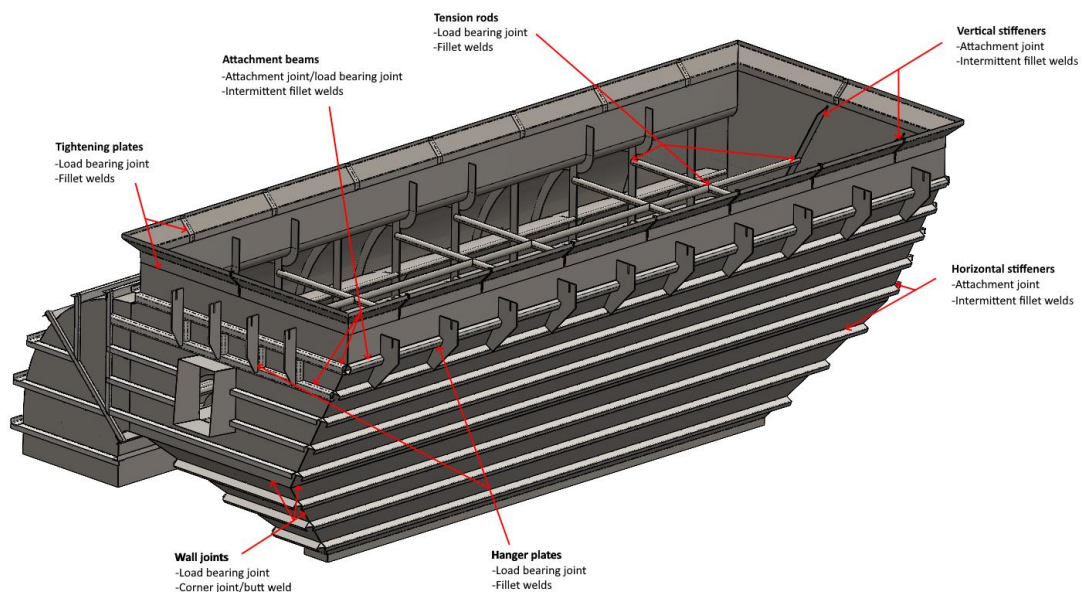


Figure 16. Introduction of different joints and joint types of an example ash hopper.

The most important weld parameter is the weld throat thickness a_w , as it has the highest contribution to the strength of the joint. Weld length L_w is another important parameter as it is also a factor defining the strength of the joint and consumption of filler metal. Both the weld length and throat thickness should be minimized to adequate size for an efficient weld. Deposited weld metal volume can be estimated by multiplying the weld cross-section area A_w with weld length L_w to compare the amount of filler metal used for each joint. Weld volume can be used as rough welding cost estimation for comparison as it reflects both the work and filler required.

SFS-EN 1993-1-8 presents two ways of assessing the weld resistance, the directional stress component method and the simplified method. In a more accurate component method, the transmitted forces by the weld are resolved into stress components of the weld. The design resistance of fillet weld is sufficient when the following equations are satisfied (SFS-EN 1993-1-8 2005, p. 43):

$$\sqrt{\sigma_{\perp}^2 + 3(\tau_{\perp}^2 + \tau_{\parallel}^2)} \leq \frac{f_u}{\beta_w \gamma_{M2}} \quad (27)$$

$$\sigma_{\perp} \leq 0.9 \frac{f_u}{\gamma_{M2}} \quad (28)$$

where σ_{\perp} is the normal stress perpendicular to the throat
 τ_{\perp} is the shear stress perpendicular to the axis of the weld
 τ_{\parallel} is the shear stress parallel to the axis of the weld
 f_u is the nominal ultimate tensile strength of the weaker part
 β_w is the correlation factor dependent on the steel grade/filler metal (table 10)
 γ_{M2} is the material partial safety factor

Both the directional method and simplified method can be used to dimension load-bearing and fixing joints, but the simplified method gives slightly more conservative results. Minimum weld throat thickness should be 3 mm and the minimum length for weld should be the larger of the conditions; 30 mm or 6 times the throat thickness (SFS-EN 1993-1-8 2005, p. 42).

Table 10. Correlation factors for fillet welds in different materials.

Steel grade	β_w
S235 P235	0.8
S275 P265	0.85
S355 P355	0.9
16Mo3	0.9
13CrMo4-5	0.9
16CrMo9-10	0.9
S420 S460	1.0

By converting the weld stress components to base material stress and rearranging the equation, the general throat thickness requirement by the directional method is obtained as (Niemi 2003, p. 70):

$$a_w \leq \frac{\beta_w \gamma_{M2} t}{2f_u} \sqrt{2\sigma_x^2 + 3\tau_{xy}^2} \quad (29)$$

Fixing welds are dimensioned based on the shear stress between the components. For horizontal and vertical stiffeners, the shear stress τ_{xy} between plate and stiffener profile can be calculated by the equation (Salmi & Pajunen 2018, p. 194):

$$\tau_{xy} = \frac{QS}{I_y t} \quad (30)$$

where Q is the statical moment of the area between stiffener profile and wall plate
 S is the shear force

By combining equations 27 and 28, the throat thickness requirement for double-sided continuous attachment weld is obtained as:

$$a_w \geq \frac{\sqrt{3} \beta_w \gamma_{M2} \cdot S \cdot Q}{2I \cdot f_u} \quad (31)$$

In a simplified method, the weld is thought to carry the load by shear independent of the force direction. The design resistance of fillet weld is adequate if, at every point of the weld, the forces per unit length transmitted by the weld satisfy the criterion (SFS-EN 1993-1-8 2005, p. 44):

$$F_{w,Ed} \leq F_{w,Rd} \quad (32)$$

where $F_{w,Ed}$ is the design value of the weld force per unit length
 $F_{w,Rd}$ is the design weld resistance per unit length

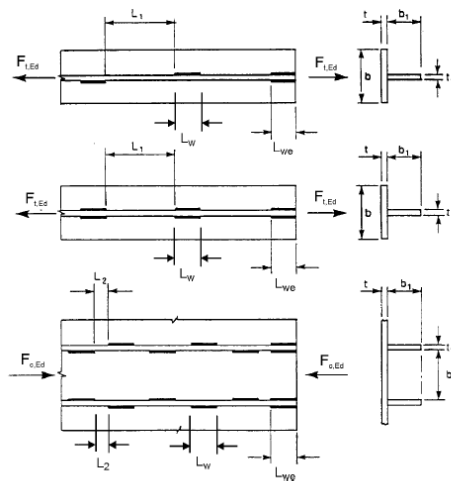
The design resistance per unit length of the weld is calculated as (SFS-EN 1993-1-8 2005, p. 44):

$$F_{w,Rd} = \frac{f_u/\sqrt{3}}{\beta_w \gamma_{M2}} \cdot a_w \quad (33)$$

Intermittent welds are an efficient way of reducing unnecessary welding on long portions where only fixing is required. Intermittent welds can be used in the hopper to attach horizontal and vertical stiffeners to plate walls. Following conditions should be met when utilizing intermittent welds:

- Intermittent fillet welds should not be used in corrosive conditions
- In an intermittent fillet weld, the gaps (L_1 or L_2) between the ends of each length of weld L_w should fulfill the requirement given in figure 17.
- In an intermittent fillet weld, the gap (L_1 or L_2) should be taken as the smaller of the distances between the ends of the welds on opposite sides and the distance between the ends of the welds on the same side
- In any run of an intermittent fillet weld, there should always be a length of weld at each end of the part connected
- In a built-up member in which plates are connected by means of intermittent fillet welds, a continuous fillet weld should be provided on each side of the plate for a length at each end equal to at least three-quarters of the width of the narrower plate

(SFS-EN 1993-1-8 2005, pp. 39-40.)



The smaller of $L_{we} \geq 0,75 b$ and $0,75 b_1$
 For build-up members in tension:
 The smallest of $L_1 \leq 16 t$ and $16 t_1$ and 200 mm
 For build-up members in compression or shear:
 The smallest of $L_2 \leq 12 t$ and $12 t_1$ and $0,25 b$ and 200 mm

Figure 17. Requirements of intermittent welds (SFS-EN 1993-1-8 2005, p. 40).

Double-sided intermittent weld can be either staggered or chained. In a chain intermittent weld, the weld beads are positioned opposite each other on the other side of the joint, and in staggered intermittent weld the bead and unwelded part alternate opposite the joint. Figure 18 presents the definition of intermittent welds. Staggered welds are favored in compression members as the unwelded part between welds is shorter and it is therefore more resistant against buckling of the connecting flange.

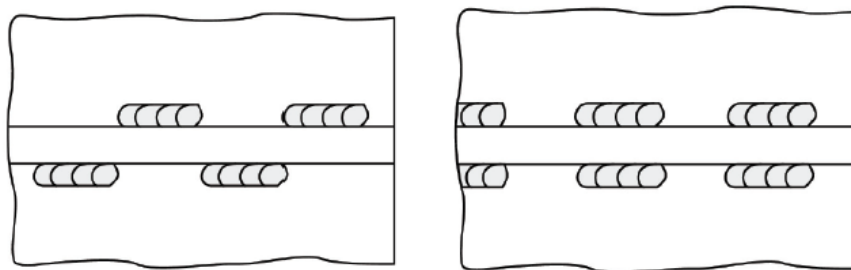


Figure 18. Staggered intermittent weld presented on the left and chain intermittent weld on the right (SFS 3052 2020, p. 42).

For intermittent welds, the actual length of the weld is considered by modifying the weld forces according to intermittent weld dimensions. Weld shear force per unit length in a single-sided intermittent weld $F_{iw,Ed}$ is modified as (SFS-EN 1993-1-8 2005, p. 46):

$$F_{iw,Ed} = F_{w,Ed} \cdot \frac{L_1 + L_w}{L_w} \quad (34)$$

Load-bearing joints are often made equal strength to the base material. Equal strength weld is a simple and safe option for joints where the loading is unclear and hard to define. Throat thickness to plate thickness ratio a_w/t for double-sided equal strength fillet weld loaded by transverse force is obtained as (Niemi 2003, p. 75):

$$\frac{a_w}{t} = \frac{\gamma_{M2}}{\gamma_{M1}} \cdot \frac{\beta_w}{\sqrt{2}} \cdot \frac{f_y}{f_u} \quad (35)$$

As the material strength is impacted by temperatures, also the weld strength is decreased by high temperatures. Weld filler metal is assumed to be at least equal strength as the base material and be reduced equally as the ultimate strength of the material is reduced in high temperatures. Base material ultimate strength in the corresponding temperature is used as the weld strength in the calculations if more detailed information is not available.

3.7 Stability

Possible loss of stability should be considered when designing compressed plate structures. A plate subjected to compressive membrane stress may lose its stability by buckling before reaching the yield strength. The buckling capacity of the plate is affected by the load, boundary conditions and the b/a dimension ratio. (Niemi 2003, p. 17.) In addition to compressive stresses, shear can cause buckling. Shear buckling occurs as the compressive principal stress causes buckling form, and the tensile stress tries to keep the plate under tension. (Niemi 2003, p. 19.)

The loads acting on the hopper walls are not globally compressive as the ash load and flue gas pressure are acting in normal of the plate and bending stress do not cause buckling. The presence of stiffeners causes local compressive stress in the wall plates, but the effect is assumed to be small. Compressive stresses are present in the stiffeners, but by selecting ready-made non-slender profiles, the local buckling can be ignored. Due to the top attachment of the hopper, the dead weight mainly causes tensile stresses in the wall panels. The hopper walls are also stiffened efficiently due to pressure loads, and the acting loads do

not generally induce buckling behavior and therefore the buckling of plates is not considered in detail in this thesis. Also, the calculation of local plate buckling in a hopper is not reasonably accurate by purely analytical methods, so it is not considered in the dimensioning tool.

The inside tension rods in the hopper are subjected to compressive forces when flue gas pressure is negative. Compressive forces can cause flexural buckling in the circular tubes and the buckling resistance of compression members should be verified as (SFS-EN 1993-1-1 2005, p. 56):

$$\frac{N_{c,Ed}}{N_{b,Rd}} \leq 1.0 \quad (36)$$

where $N_{c,Ed}$ is the design value of compressive force
 $N_{b,Rd}$ is the buckling resistance of the member

The design value of compressive force is not a direct external force so the force acting on the tension rods can be estimated by simplified analytical calculation or by FEA as defined in chapter 3.4. The sizes of circular tubes used as tension rods vary but all profiles fall in the cross-section classes 1-3 and therefore the whole cross-section area can be considered effective. The buckling resistance for cross-section classes 1, 2 and 3 is then calculated by (SFS-EN 1993-1-1 2005, p. 57):

$$N_{b,Rd} \leq \frac{\chi A f_y}{\gamma_{M1}} \quad (37)$$

where γ_{M1} is a partial safety factor for resistance of member
 χ is the reduction factor for the relevant buckling curve
 A is the cross-sectional area of the member

The reduction factor for the relevant buckling curve is obtained by equation, where Φ is an intermediate factor and $\bar{\lambda}$ is non-dimensional slenderness (SFS-EN 1993-1-1 2005, p. 57):

$$\chi = \frac{1}{\phi + \sqrt{\phi^2 - \bar{\lambda}^2}} \leq 1 \quad (38)$$

The intermediate factor for determining the reduction factor is calculated by equation, where α is an imperfection factor (SFS-EN 1993-1-1 2005, p. 57):

$$\phi = 0.5[1 + \alpha(\bar{\lambda} - 0.2) + \bar{\lambda}^2] \quad (39)$$

The imperfection factor is determined by the buckling curve and it takes into account the geometrical imperfections and initial deflection of the profile. Table 11 presents corresponding imperfection factors for different buckling curves. Circular tubes are cold-formed hollow sections and therefore c is the appropriate buckling curve (SFS-EN 1993-1-1 2005, p. 58). Buckling curve c takes into account local bow imperfection of $L/200$, which is adequate to cover the initial deformation due to dead weight (SFS-EN 1993-1-1 2005, p. 34).

Table 11. Imperfection factors for buckling curves (SFS-EN 1993-1-1 2005, p. 57).

Buckling curve	a_0	a	b	c	d
Imperfection factor α	0.13	0.21	0.34	0.49	0.76

The non-dimensional slenderness $\bar{\lambda}$ of the member is calculated by equation (SFS-EN 1993-1-1 2005, p. 57):

$$\bar{\lambda} = \sqrt{\frac{Af_y}{N_{cr}}} = \sqrt{\frac{f_y}{f_{cr}}} \quad (40)$$

where N_{cr} is the elastic critical force for the relevant buckling mode
 f_{cr} is the critical buckling stress for the relevant buckling mode

The elastic critical buckling force can be calculated by the Euler equation, where L_n is the buckling length of member dependent of boundary conditions (Salmi & Pajunen 2018, p. 277):

$$N_{cr} = \frac{\pi^2 EI}{(L_n)^2} \quad (41)$$

The stability can also be verified by FEA, but analytical calculations are needed for the dimensioning tool.

3.7.1 Effect of temperature on the stability

The buckling capacity of a member is reduced in high temperatures as the slenderness is modified due to altered yield strength to Young's modulus ratio at elevated temperatures. Reduction to buckling capacity is considered by reduced material properties. The buckling resistance in a fire situation, at temperature, is calculated as (SFS-EN 1993-1-2 2005, p. 29):

$$N_{b,fi,Rd} \leq \frac{\chi_{fi} A k_{y,\theta} f_y}{\gamma_{M,fi}} \quad (42)$$

where χ_{fi} is the reduction factor for flexural buckling in the fire design situation
 $k_{y,\theta}$ is the reduction factor for yield strength of steel at a temperature
 $\gamma_{M,fi}$ is the partial safety factor for resistance of member, at temperature

The term $k_{y,\theta} f_y$ can be simplified directly to yield strength at corresponding temperature $f_{y,\theta}$ as the material properties are available. The reduction factor for flexural buckling in the fire design situation χ_{fi} is calculated by equation, where Φ_θ is an intermediate factor at temperature and $\bar{\lambda}_\theta$ is non-dimensional slenderness at temperature (SFS-EN 1993-1-2 2005, p. 29):

$$\chi_{fi} = \frac{1}{\Phi_\theta + \sqrt{\Phi_\theta^2 - \bar{\lambda}_\theta^2}} \leq 1 \quad (43)$$

The intermediate factor at temperature for determining the reduction factor is calculated by equation (SFS-EN 1993-1-2 2005, p. 29):

$$\Phi_\theta = 0.5 \left[1 + \alpha \bar{\lambda}_\theta + \bar{\lambda}_\theta^2 \right] \quad (44)$$

The imperfection factor α for cold-formed members at a temperature modifies to (SFS-EN 1993-1-2 2005, p. 29):

$$\alpha = 0.65 \sqrt{235/f_y} \quad (45)$$

The non-dimensional slenderness at temperature $\bar{\lambda}_\theta$ is modified according to reduced material properties as follows (SFS-EN 1993-1-2 2005, p. 29; Gunalan, Heva & Mahendran 2014, p. 157):

$$\bar{\lambda}_\theta = \bar{\lambda} \sqrt{\frac{k_{y,\theta}}{k_{E,\theta}}} = \sqrt{\frac{f_{y,\theta} A_{eff}}{f_{cr,\theta} A}} \quad (46)$$

where $k_{E,\theta}$ is the reduction factor to the linear elastic range
 $f_{cr,\theta}$ is the critical buckling stress for the relevant buckling mode at a temperature

In addition to reduced buckling capacity, high temperatures can also affect stability by increased compressive forces. Additional compressive stresses are introduced if the thermal elongation of the structural member is constrained. Therefore, it is also important to allow free thermal elongation and have even temperature distribution between components.

3.8 Erosion, abrasion and corrosion

Flowing particles in the hopper can cause wear in the inside surfaces by abrasion or erosion. The conditions inside a hopper can also be corrosive especially in the recovery boilers. The possible effects of wear should be included in the design and allowance for material loss should be taken in the effective plate thickness. Also, the manufacturing tolerances of plate thickness should be considered. The walls in contact with the particles should be assumed to lose an amount of wall thickness during the lifetime of the structure and it should be considered with wear allowance Δt_a . (SFS-EN 1993-4-1 2007, p. 27.)

3.9 Design details

Various design details like the connection between components are repeated in hoppers of different scales. Design details can be ignored in the simplified calculation as the details are generalized and generally designed strong enough. Manholes should be adequately stiffened according to internal design instructions, so the local effects can be ignored in the general calculation. Plates and additional stiffeners are used to support manholes by its edges. The attachment of flue gas duct and hopper corners are made equal strength and with sufficient stiffening. The ash conveyor is attached to the bottom of the hopper using a standardized flange connection. The strength of details for general case is verified using FE-analysis.

4 FE-ANALYSIS

Finite element analysis is used as the numerical analysis tool for global analysis of the hopper and to verify the use of simplified analytical calculation. Structural analysis is done with Ansys Mechanical 2021 R1. Linear static analysis (LA) is used as the general analysis type and additionally geometrically non-linear analysis is used (GNA) to verify results. Stability is checked by simple linear buckling analysis (LB).

4.1 Material

Material properties vary based on the design temperature and the corresponding material properties presented in chapter 2.5 are utilized. Linear-elastic material model is used in FE-analysis.

4.2 Geometry and elements

The FE-analysis in this thesis focuses on one reference hopper geometry, and general conclusions are applied to other hopper geometries. The hopper 3D-geometry is pre-processed into a midsurface model. All the plate parts are modeled with plate elements and tension rods are modelled with beam elements. The weights of surrounding structures are modeled with mass elements. The whole geometry of the hopper is used for the global analysis and individual stiffened plate sections with different b/a -ratios are analyzed separately. Figures 19 and 20 present the geometry and mesh of a general hopper structure and example stiffened plates with different b/a -ratios.

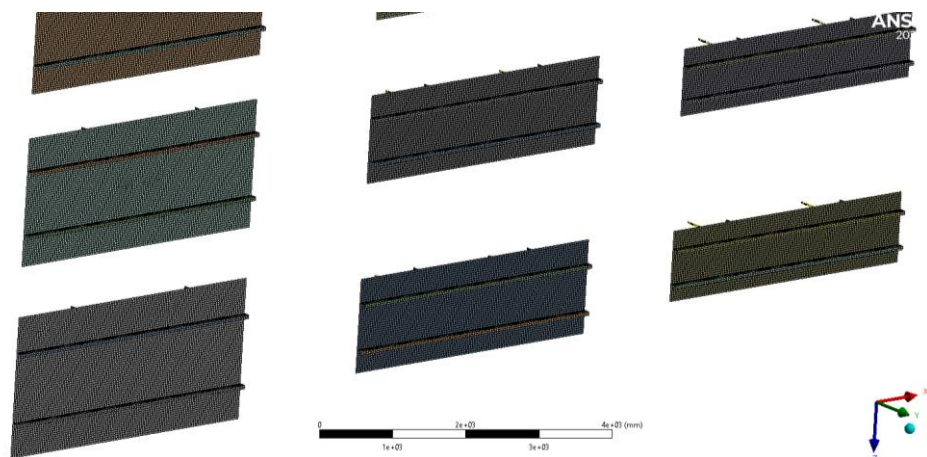


Figure 19. General geometry and mesh of the analyzed stiffened plates.

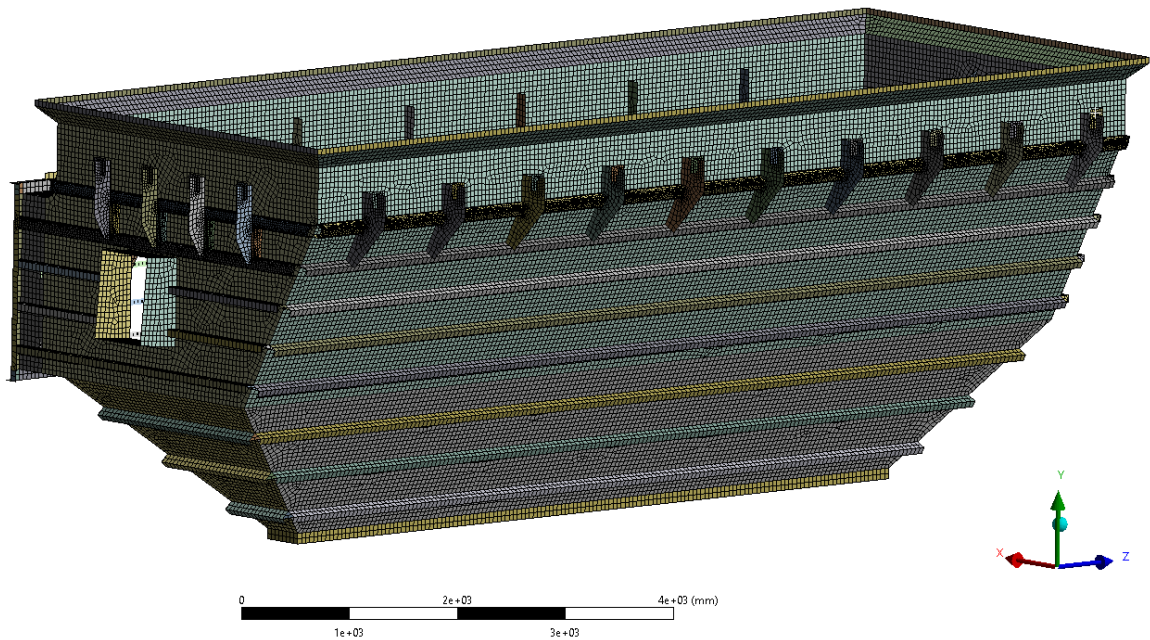


Figure 20. General geometry and mesh of the ash hopper.

4.3 Loads and boundary conditions

Load combinations presented in chapter 2.5 are used in the analysis of the whole hopper structure. For the analysis of individual stiffened plate segments, design pressure load is used. Fixed boundary condition is set to the attachment plates and to the top edge of the hopper. A rigid element is used between the bottom edges of the hopper to consider the stiffness of the conveyor flange connection. Symmetry to the x-axis is set to the cut plane of the flue gas duct. In the analysis of stiffened plates, pinned boundary conditions are set in the tension rod ends placed at the stiffener junctions. Symmetry is additionally utilized in all the cut edges of the plates.

5 ANALYSIS AND OPTIMIZATION OF THE DESIGN

Based on the design criteria, a preliminary analysis of the general hopper was done to study the structural behavior and locate key structural details. The obtained results are used as the approach for optimizing the design. Different options for various details are compared to find the best construction. Simplifications are studied and the simplified calculations are compared to FEA results to verify the use of methods. Dimensioning tool can then be created based on the results of the analysis.

5.1 Simplifications

Ash hopper is not meant for storage of large amounts of solids unlike silos, so the silo loads are not explicitly applicable for an ash hopper. Relatively small amounts of ash may accumulate in the hopper, and therefore the load distribution and particle flow differ from a tall storage silo. Support construction of ash hoppers and silos are also different as silos are usually supported from the bottom and ash hopper is attached from the top. Therefore, the friction traction of particles do not cause compressive stress in the ash hopper walls, which could induce buckling.

The calculation of silo load components is complex and setting the calculated load components to segments of structure is laborious, so the silo load components were replaced by simple hydrostatic pressure load. Arbitrary comparison of different loads was done by FEA to validate the use of the simple method. As can be seen from figures 21 and 22, the general von Mises stress is nearly equal with both methods. Used hopper angles for smaller walls are 30° and 35° for larger walls and applied loads are the flue gas pressure and ash loads.

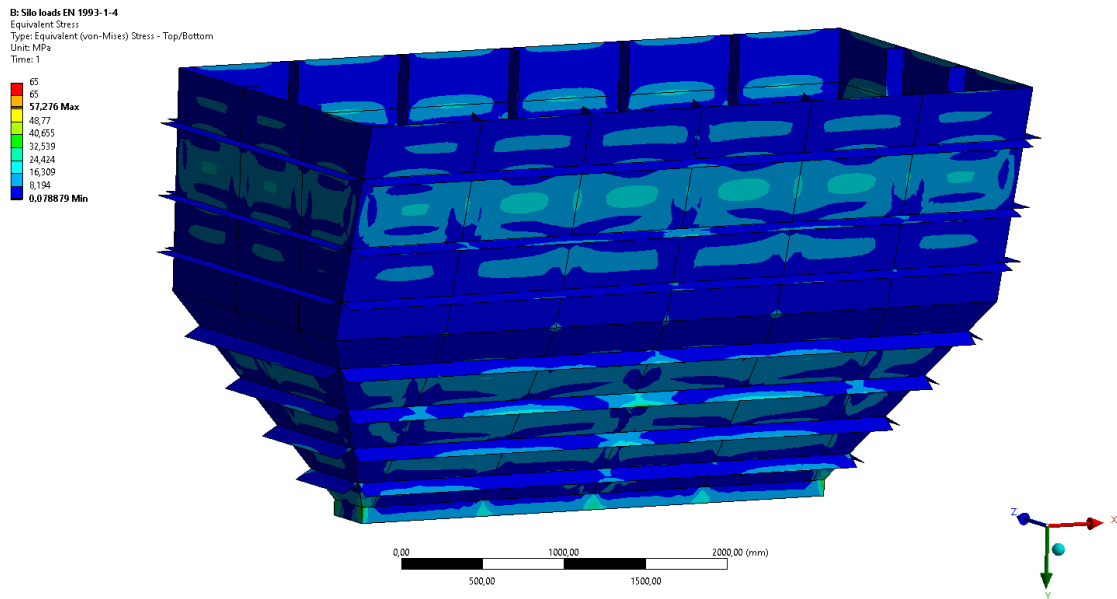


Figure 21. Silo loads according to SFS EN 1991-1-4.

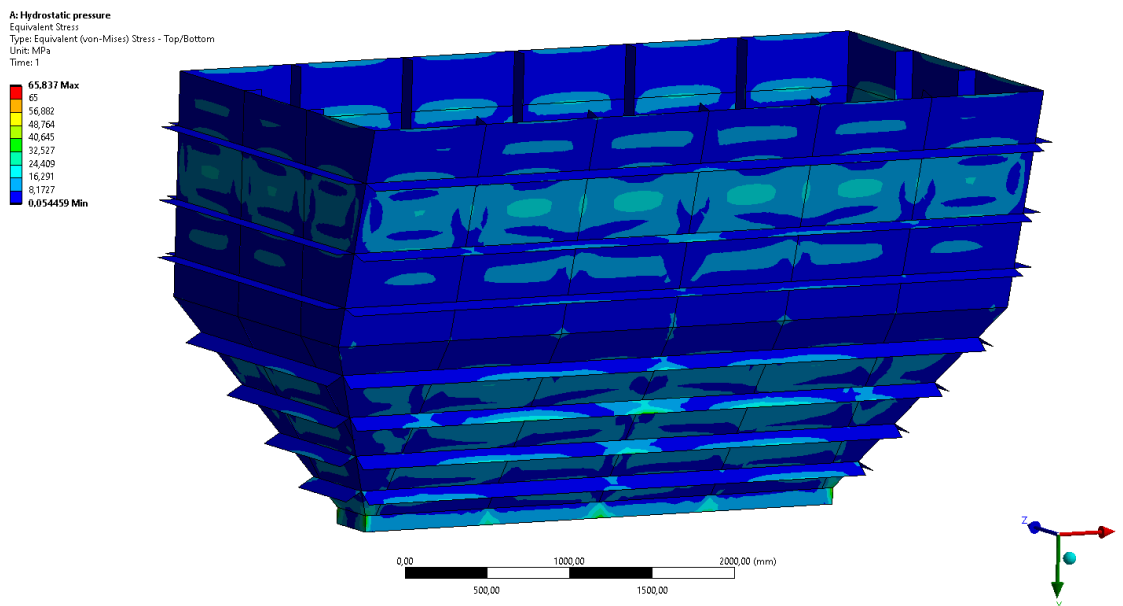


Figure 22. Hydrostatic pressure load.

Hopper angle defines the ratio between load components, and a steeper angle causes more friction traction. Figure 23 presents the plotted ratio of load components relative to hopper angle. Typically, the hopper angles are between $30 - 45^\circ$, so the friction traction will only contribute to less than 0.5 of the normal pressure. Friction traction will mainly cause tensile stress, which plates can endure greatly.

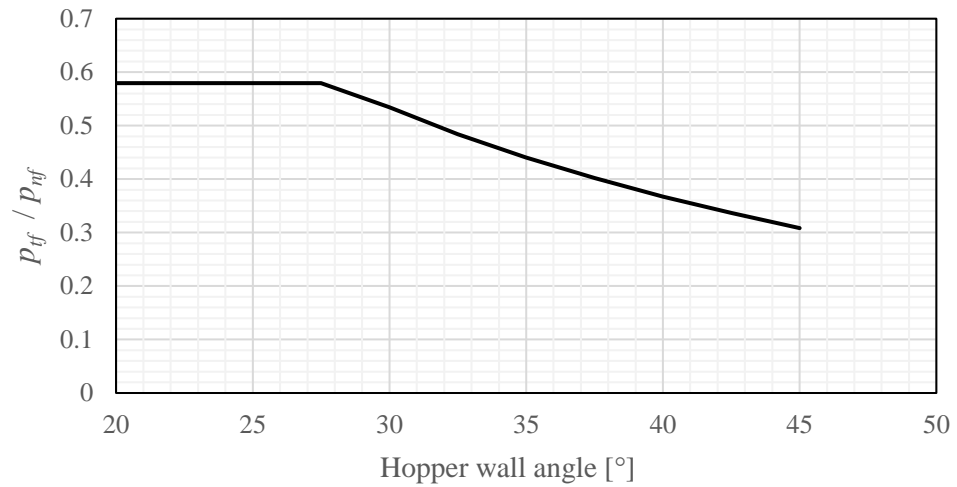


Figure 23. The ratio of friction traction p_{tf} and normal pressure p_{nf} relative to hopper angle.

5.2 Analysis and optimization of stiffened plates

Plate behaviour in a continuous stiffened panel was examined to verify made assumptions. Membrane stresses and shear stresses were obtained from the front wall of the hopper to study the effect of stiffeners in the individual plate segments. As the small deflection theory only assumes bending stresses are present in a plate and no shear stresses occur, the validity of this assumption in a continuous stiffened plate was considered. Figures 24 and 25 present the normal stress distributions in Z- and Y-directions of the front wall and figure 26 presents the in-plane shear stress along the front wall. Stresses are obtained from the middle of the plate elements.

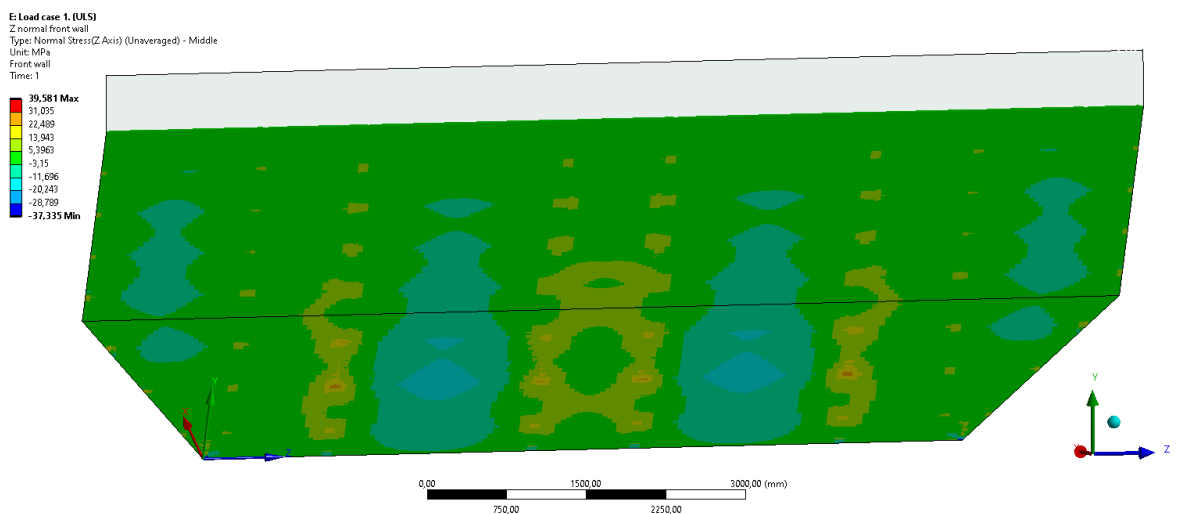


Figure 24. Z-normal stress σ_z of stiffened hopper front wall panel in the midplane of plate element (membrane stress).

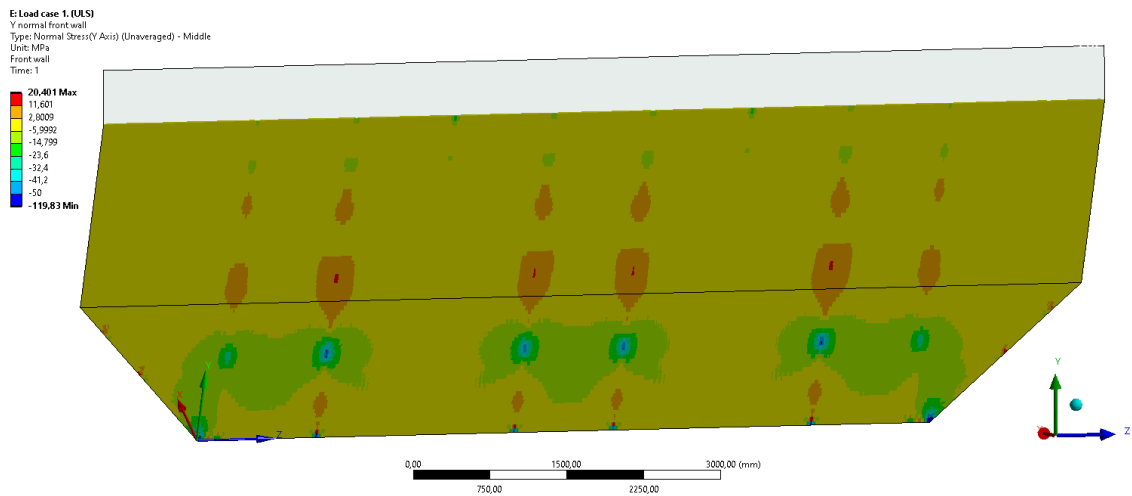


Figure 25. Y-normal stress σ_y of stiffened hopper front wall panel in the midplane of plate element (membrane stress).

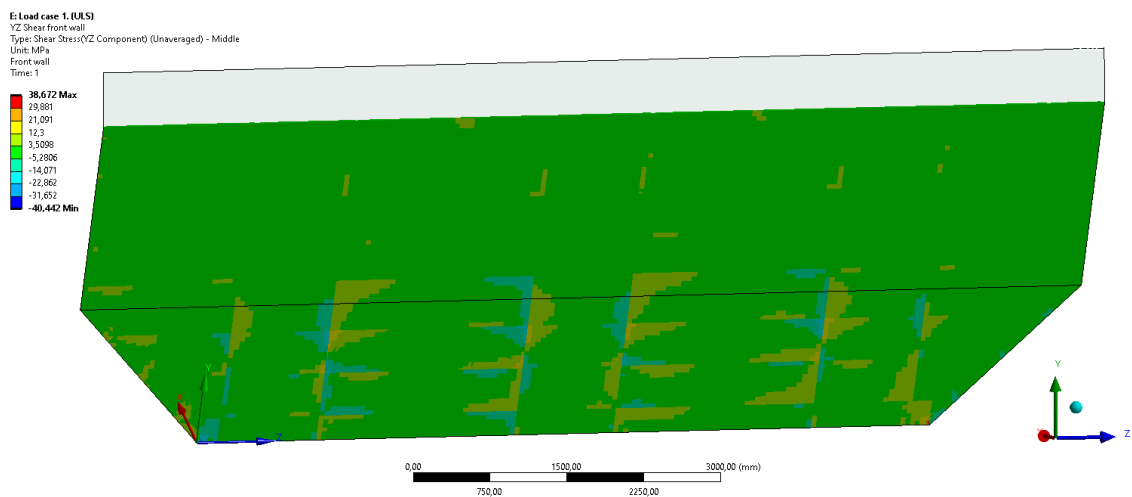


Figure 26. In-plane YZ-shear stress τ_{yz} of stiffened hopper front wall panel in the midplane of plate element.

The general membrane stresses of the wall panel are small or non-existent as according to the theory. However, minor in-plane normal stresses occur in the vicinity of stiffeners due to their effect. When considering a plate segment near stiffener, the stiffener and effective width of the wall panel on each side work as a combination profile, and the neutral axis is lifted up from the middle of the plate accordingly. Then as the stiffener bends, the bending stress of combination profile is seen as in-plane normal stress at the middle of the plate element. Stress distribution also shows the locations and importance of tension rods inside. Individual plate segments are clearly distinguished by the shear stress distribution as shear only occurs at the stiffeners.

Stress components of a single plate segment were plotted along the length of the longer side for further analysis. Arbitrary plate surrounded by stiffeners was chosen and stress results read along 2 lines: at the edge of the longer side and at the middle of the plate between horizontal stiffeners (figure 27). Mesh is refined at the edges as the stress gradient is assumed to be high. All stress results are read from the middle of the plate-element. Figure 28 presents the z-normal stress distribution and figure 29 presents the in-plane shear distribution along the length of the plate.

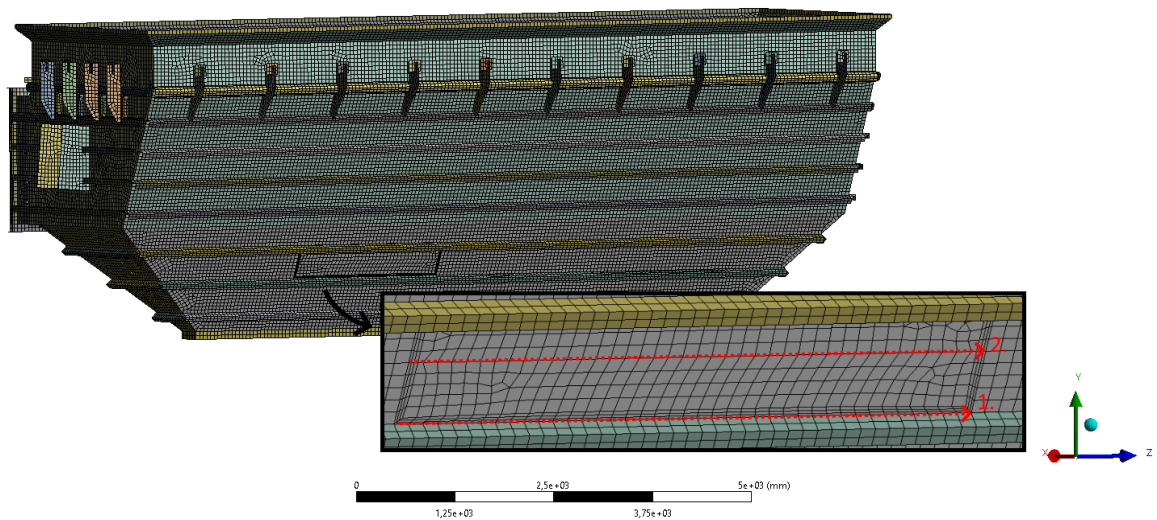


Figure 27. Obtaining of stress components from plate segment surrounded by stiffeners.

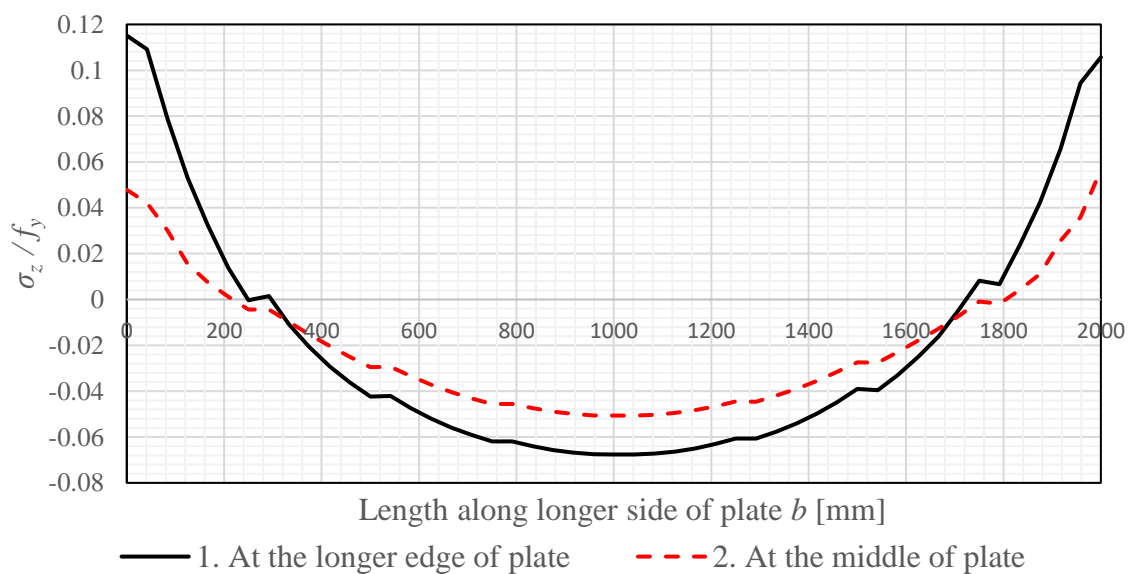


Figure 28. Z-normal stress σ_z normalized to yield strength f_y along the length of the plate segment.

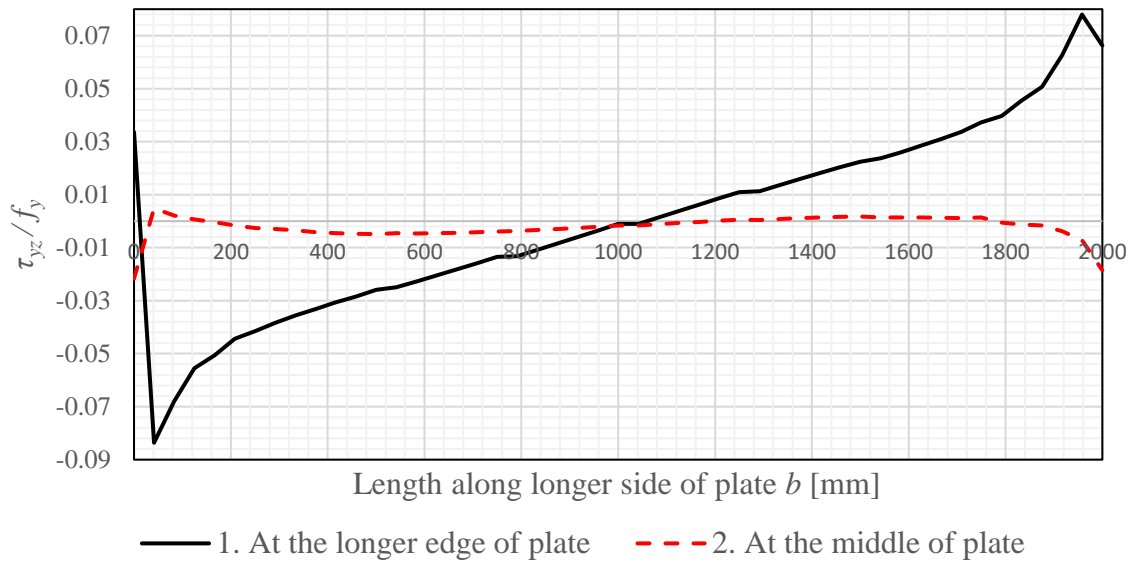


Figure 29. In-plane YZ-shear stress τ_{yz} normalized to yield strength f_y along the length of the plate segment.

Membrane stresses along the length of the plate segment are relatively small in general. Tensile stresses occur at both ends of the longer side and compressive stress between ends. Maximum tensile stress is considerably higher compared to compressive stresses. Bending of stiffener at boundaries causes the membrane stresses in the plate. Compressive stresses only occur locally and are minor and therefore plate buckling is not considered to be a determining phenomenon. Plate shear stresses peak at the corners of the plate where the stiffeners intersect as the stiffeners form rigid support and vanish at the centerline of the plate as assumed. Shear stresses only occur directly at the stiffeners. Overall shear stresses in the plate are small as assumed by the plate theory and it is valid to use it in the stress analysis of single stiffened plates.

Different boundary conditions were tested and compared with FEA results to verify the use of correct boundary conditions and assess the accuracy of analytical methods. Boundary conditions are compared with FEA results of a stiffened plate within a continuous plate wall (figure 30). Figure 31 presents the plate stress calculated with different boundary conditions and methods and figure 32 presents the corresponding deflections. All presented stresses are equivalent von Mises stresses.

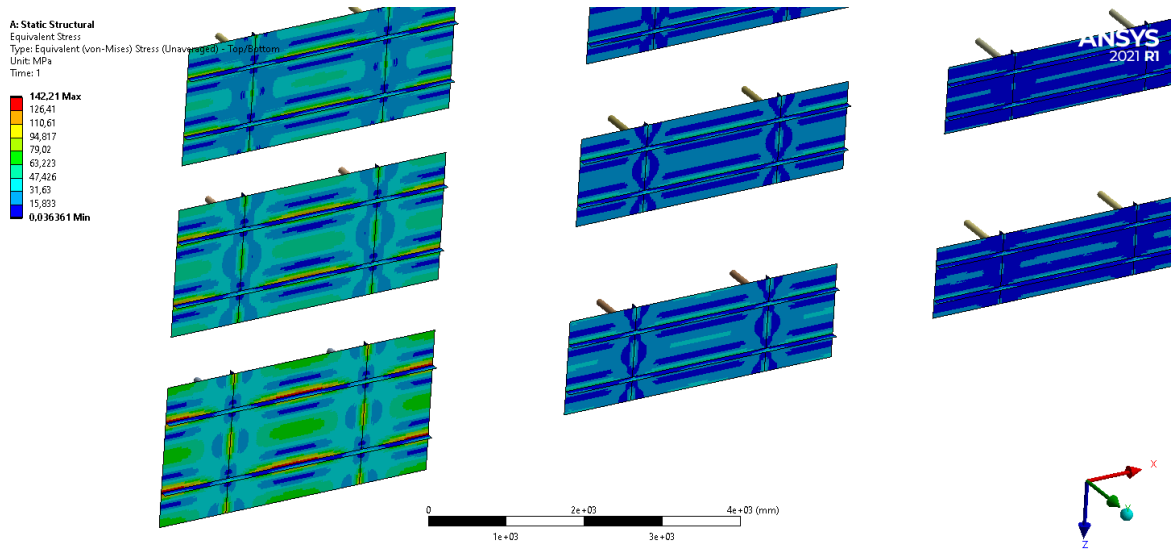


Figure 30. Von Mises stress of general stiffened plates analyzed with FEA.

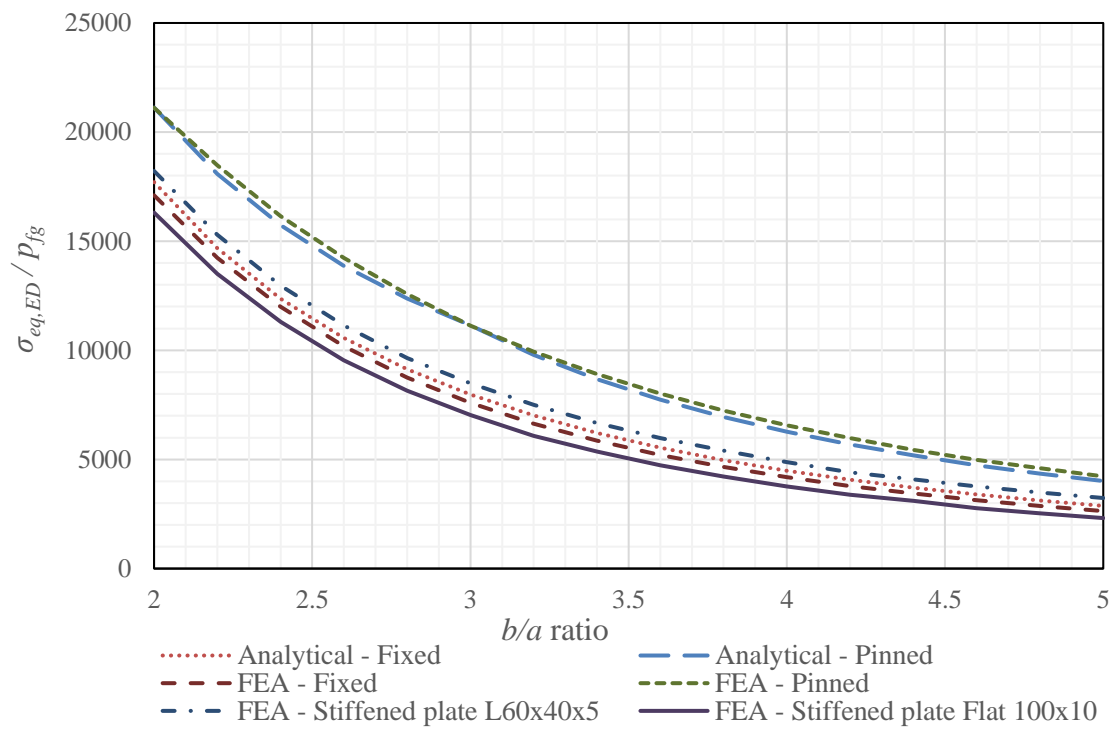


Figure 31. Maximum von Mises stress of plate $\sigma_{eq,Ed}$ normalized to applied flue gas pressure p_{fg} with different b/a ratios ($b = 2000$ mm, $a =$ variable).

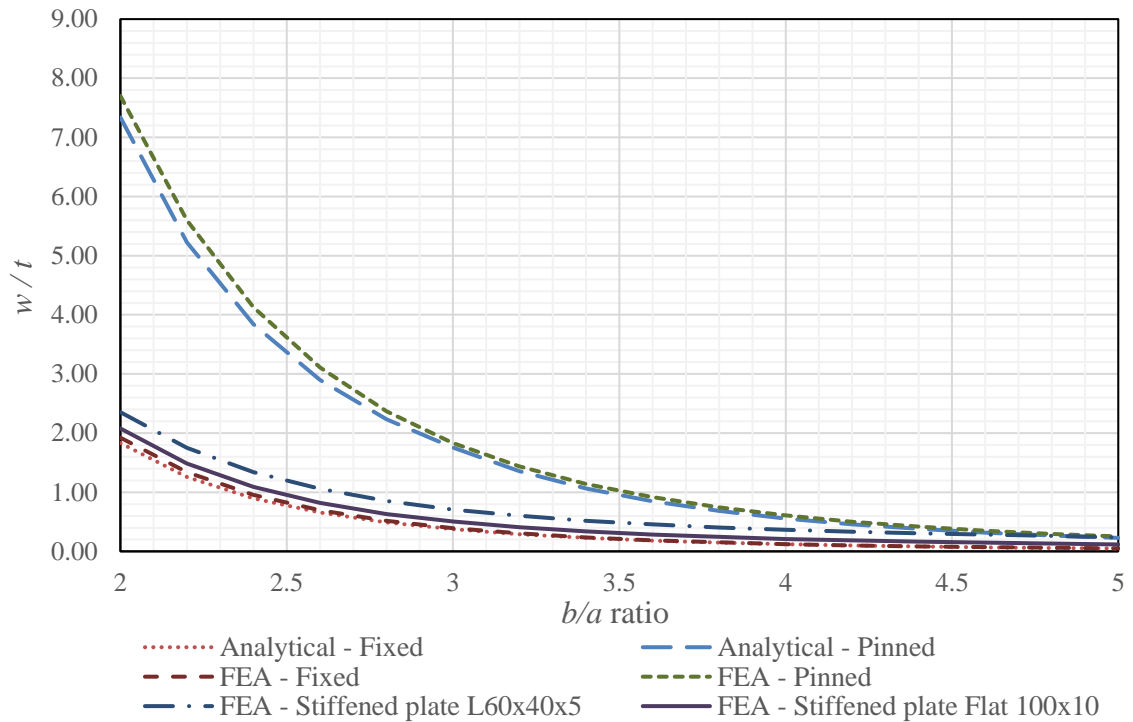


Figure 32. Deflection of plate segment w normalized to plate thickness t with different b/a ratios ($b = 2000$ mm, $a =$ variable).

The maximum von Mises stress in a pinned plate occurs at the center of the plate and for rigidly supported and stiffened plates at the edge of the long side. Analytical and numerical methods produce relatively matching results. Differences with corresponding stresses are mostly due to numerical error and measurement inaccuracy from the mesh sizing. Rigid boundary conditions match the stress of stiffened plate the best as assumed.

The plate stiffened by L-profile has slightly higher stress compared to the flat-stiffener due to added stress by the eccentricity of the center of gravity and torsion center. Compared to analytical calculation with fixed boundary conditions, the plate stress with L-profile is 5-10 % higher and with a flat stiffener, the plate stress is 10-15% less than the analytically calculated stress. Analytical calculation gives conservative results for plate stress with symmetrical stiffener profiles but can give slightly non-conservative results when considering asymmetrical stiffeners.

Standards present two ways of assessing the effective width of the plate wall connected to a stiffener. A comparative study was made to verify the use of the method and study the

difference between a FEA-model of stiffened plate. Figure 33 presents the maximum stress of stiffener connected to a plate segment and figure 34 presents the corresponding deflections. Stiffener length is equal to the longer side of plate b and the shorter side of plate a is kept as constant. The stress of stiffener increases in a square of the length b and linearly with side length a .

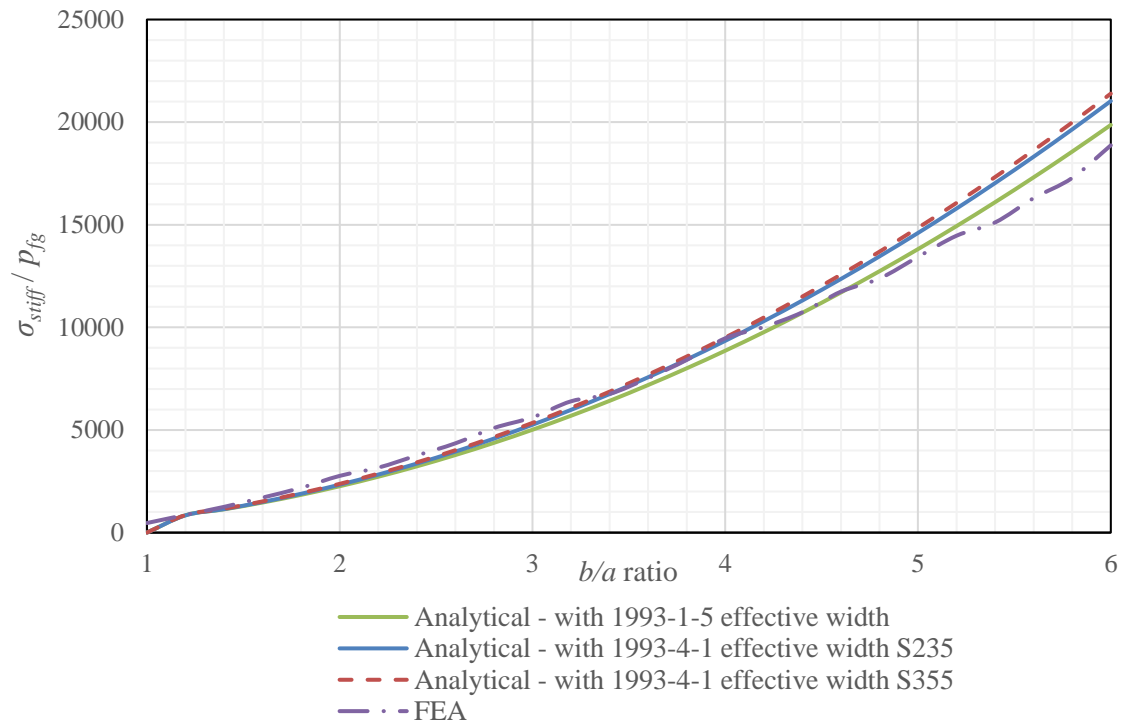


Figure 33. Stiffener bending stress σ_{stiff} normalized to applied flue gas pressure p_{fg} with different b/a ratios ($a = 450$ mm, $b =$ variable).

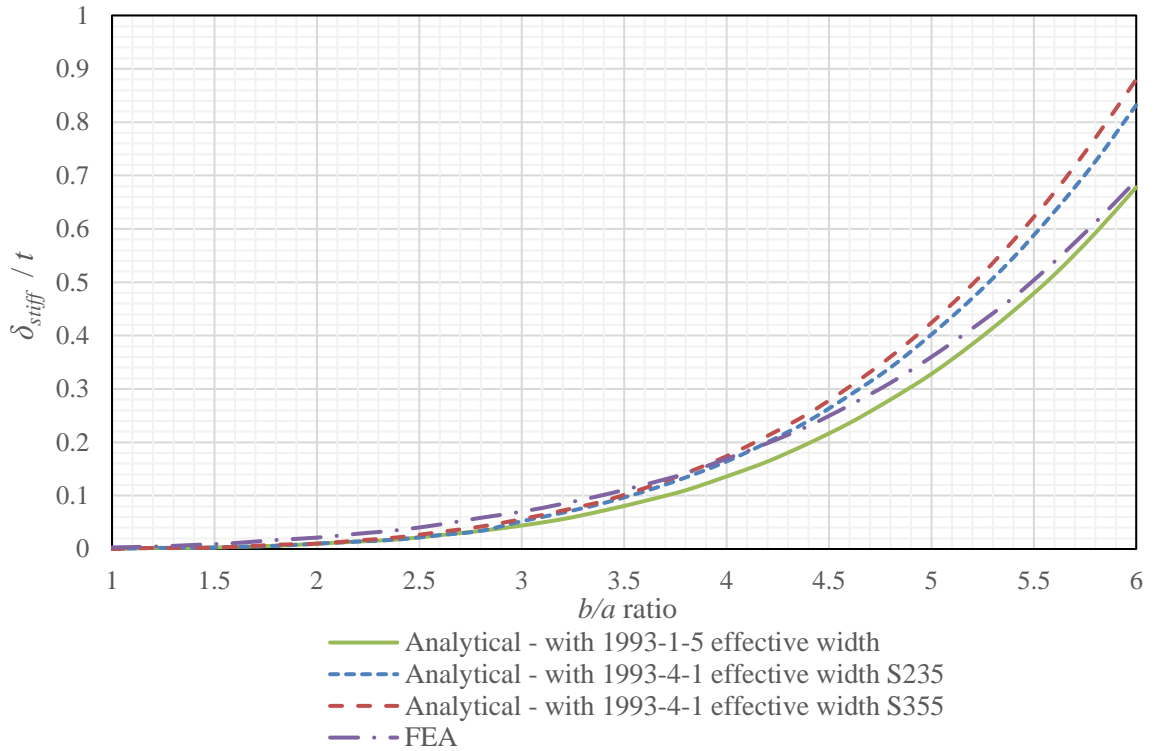


Figure 34. Stiffener deflection δ_{stiff} normalized to plate thickness t with different b/a ratios ($a = 450$ mm, $b =$ variable).

By using the effective width defined in SFS-EN 1993-4-1, both the stress and deflection are slightly conservative comparing to FEA results. With the effective width defined in SFS-EN 1993-1-5, the results are a better match to FEA however the stress and especially deflection are underestimated slightly in some cases. The calculation of effective width by this method also requires dimensions that are variables so the calculation would have to be iterative. Effective width defined in SFS-EN 1993-4-1 is simple to calculate and gives more conservative results, so it is better to use in a dimensioning tool.

The optimal layout of stiffeners is based on the concept that plate stress and stiffener stress are equal to the corresponding design strengths with certain plate width and stiffener length. Then the plate and stiffener both contribute equally to bearing the load and one does not exceed design strength before the other. Both the length and width should be maximized with the correct b/a -ratio to achieve the layout with the least number of stiffeners. The optimal b/a -ratio is constrained by all dimension variables and the solution is a compromise between plate stress, stiffener stress and other design constraints. The stress of stiffener increases exponentially as the side length b is increased and plate stress increases exponentially

as the side length a is increased. Additionally, the stress of stiffener increases linearly as side a is increased and plate stress increases linearly and according to coefficients as side length b is increased. As both plate dimensions affect the plate stress and stiffener stress, both variables a and b have to be solved simultaneously. The correlation of dimensions to stress is also non-linear, therefore the optimal dimensions are obtained iteratively for each stiffener profile, plate thickness and design strength at the corresponding temperature. The optimal length for a stiffener in plate segment is first iteratively solved based on the design strength $f_{y,Ed}$ by rearranging and modifying equation 22:

$$b = \sqrt{\frac{12Wf_{y,Ed}}{pa}} \quad (47)$$

As dimension a is also needed in the calculation, plate stress and stiffener stress with different b/a -ratios are also calculated simultaneously to search for a b/a -ratio with the plate stress is below the material strength. The dimension a can then be solved for equation 47 by b and valid b/a -ratio. The iteration loop is calculated using MS Excel. The final result from the iteration is the maximum dimension for b and the corresponding optimal b/a -ratio with both the stiffener stress and plate stress are below or equal to the design strength. Stiffener length can also be set manually and the corresponding b/a ratio for plate then obtained respectively.

5.3 Optimization of the design

Welding is a large part of the manufacturing of the hopper. All weld joints of an example hopper were examined to assess what are the most laborious components and where possible improvement can be made. Estimates of weld volumes were calculated for each joint and then categorized for different components. Table 12 presents calculated values and figure 35 illustrates the distribution of welding workload between components.

Table 12. Calculated weld lengths and volumes for components of the ash hopper.

Summary	Weld volume [mm ³]	% of total	Weld length [mm]	% of total
Horizontal stiffeners	1154400	24.97	63150	23.59
Vertical stiffeners	377600	8.17	23600	8.81
Hanger plates	801600	17.34	20300	7.58
Attachment beams	430400	9.31	26900	10.05
Tightening plates	432000	9.34	27000	10.08
Tension rods	452800	9.79	28300	10.57
Wall joints	974749	21.08	78504	29.32
TOTAL	4623549	100	267754	100

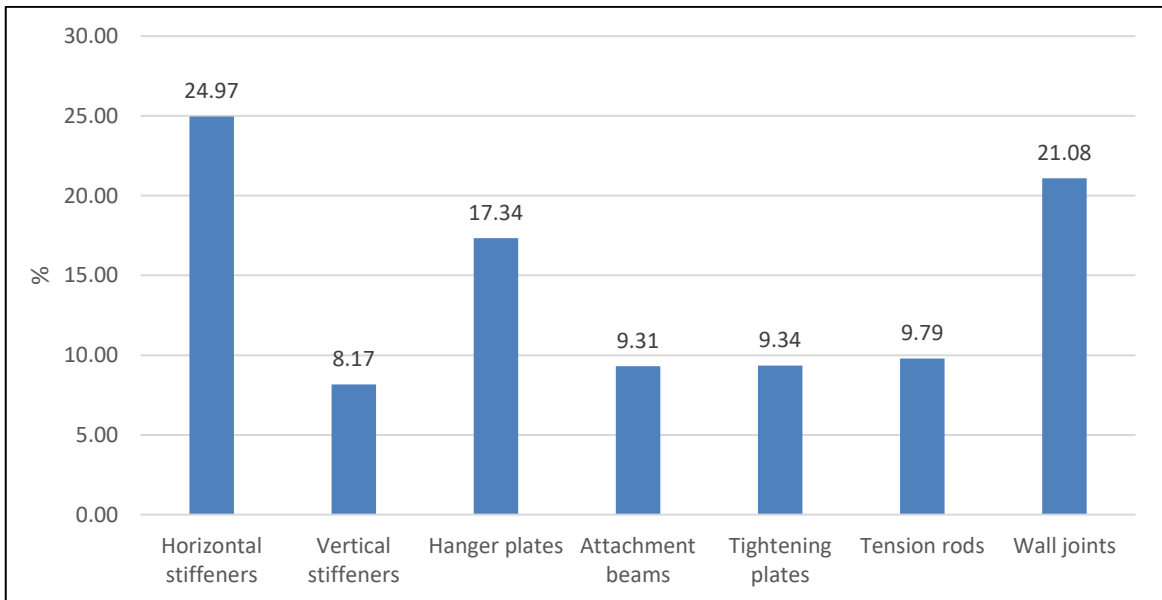


Figure 35. The relative amount of weld volume used for different components of an example ash hopper.

As can be seen from figure 35, the largest amount of welding is related to the attachment of horizontal stiffeners. There is also a lot of welding in the hanger plates as there are multiple long seams of equal strength welds. The possibility of reducing the number of hanger plates should be additionally studied. The amount of welding in tension rods can be significantly reduced by an alternative joining method of crossing rods. For some components like wall joints, the amount of welding cannot be reduced.

The welding of horizontal and vertical stiffeners is a large part of the total welding. Different options for the intermittent welds were examined to validate the best option. By using staggered intermittent welds, total weld volume can be lower than with chain intermittent welds,

according to the required dimensions defined in figure 17. Staggered welds are also recommended in members subjected to compression and as the flue gas pressure can be negative or positive, welds on both sides can be subjected to compression. The throat thickness requirements need to be considered case-by-case. Intermittent welds should only be considered when the throat thickness requirement for continuous weld is less than 3 mm.

As mentioned, the welding of stiffeners to walls is a major part of the hopper assembly. By use of stiffeners the thin walls can be strengthened to carry the required loading. The possibility of reducing the number of stiffeners and welding by the use of thicker plates was examined. Thicker plates need less stiffening, but they add more overall weight and are more expensive compared to a thinner sheet.

The effect of plate thickness on the required number of stiffeners was first studied by simple analytical equations of transversely loaded plates presented in SFS-EN 1993-1-7. As can be observed from equations 7-8, the plate thickness t is in the power of 2, meaning that when plate thickness is doubled the stress is reduced by a factor of 4. In other words, it also results that a single plate segment can have 4 times the area A_p and the number of stiffeners in both vertical and horizontal directions can be theoretically halved when the thickness is doubled. Theoretically calculated effect of plate thickness only considers the plate stress of a single plate segment, and it ignores other local effects, therefore it can only be used as an approximation. FEA comparison of 4 mm wall with equally spaced stiffeners and 8 mm wall plate with half the stiffeners was conducted for verification. Figure 36 presents the von Mises stress with 4 mm plate walls and figure 37 with 8 mm plate walls. Nominal plate thicknesses are used in the comparison.

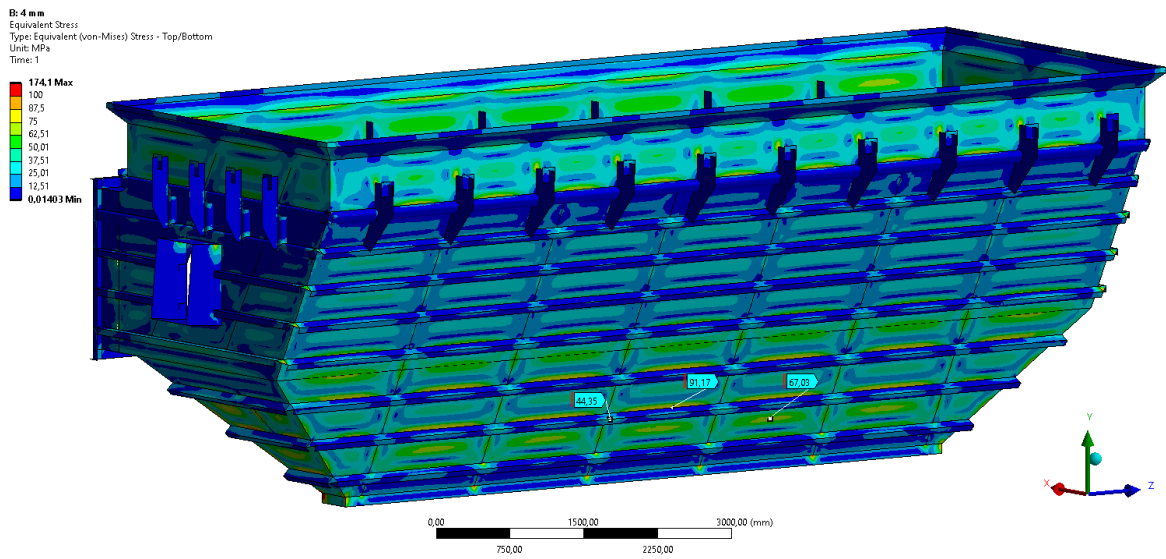


Figure 36. Ash hopper von Mises stress with 4 mm plate walls and equidistant stiffeners.

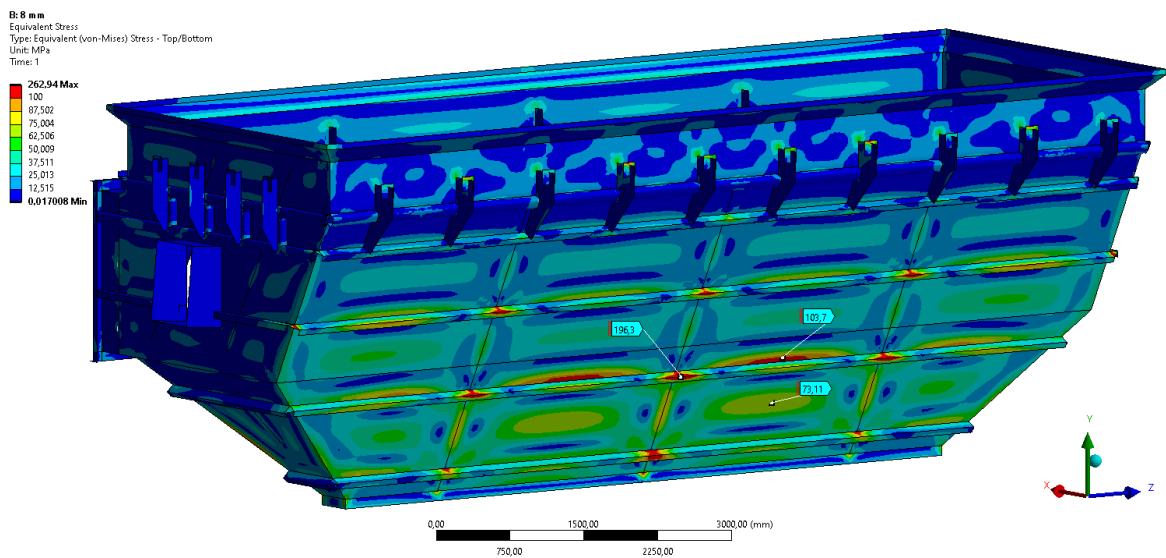


Figure 37. Ash hopper von Mises stress with 8 mm plate walls with half the stiffeners.

The stress of plate segments between models is relatively similar as according to analytical calculation, but the stress in the larger segment of 8 mm plate is slightly higher. Peak stresses are increased overall as the support lengths are increased. When the stiffener length in the plate section is doubled, the stress of stiffeners is roughly quadrupled. The stiffener profile should then be also changed accordingly to account for longer support lengths which further increases the total mass. Results show that the analytical comparison of plate thicknesses provide a good approximation, but in reality, the number of stiffeners cannot be reduced in direct correlation due to additional local effects.

Correlation of plate thickness to required amount stiffeners and its effect on costs and properties was studied with the example hopper. Values are approximated by calculation with simple plate equations and then modifying the 3D model accordingly. Table 13 roughly illustrates the effect of changing the plate thickness on the most important hopper properties. Plate thickness of 4 mm is used as the baseline for comparison. Due to geometrical constraints, the placement of stiffeners is not exact with calculated distances and the presented thickness comparison is only valid for the example hopper.

Table 13. Calculated estimated effect of plate thickness on the hopper properties.

Summary	Change in total weight %	Change in stiffener profile needed %	Change in total weld volume %
4 mm plate	0.00	0.00	0.00
5 mm plate	+4.1	-19.3	-5.6
6 mm plate	+9.9	-32.9	-9.6
8 mm plate	+25.1	-46.0	-13.3

The final optimal plate thickness varies on the material and labor costs. However, the total weight is one of the most important factors affecting the total cost, so therefore thinner plates are the more optimal solution in terms of cost. Calculation plate thickness of 5 mm or 4 mm is generally the most favorable choice for the hopper walls.

The tension rods carry the load by axial force and the rod profile is selected based on the adequate flexural buckling resistance under negative pressure. The boundary conditions and member length are the most important factors in flexural buckling capacity. Crossings of the perpendicular tension rods form support points where the buckling length is effectively reduced. However, there are no major forces in the joints of the crossing rods, so welded X-joint is not necessary. Different options for joining the crossing rods were designed to reduce the amount of cutting and welding of the rods (figure 38). With separate connectors, the weld joint types also change from load-bearing joint to binding joint as the joint only provides support in the event of loss of stability or excessive deformation.

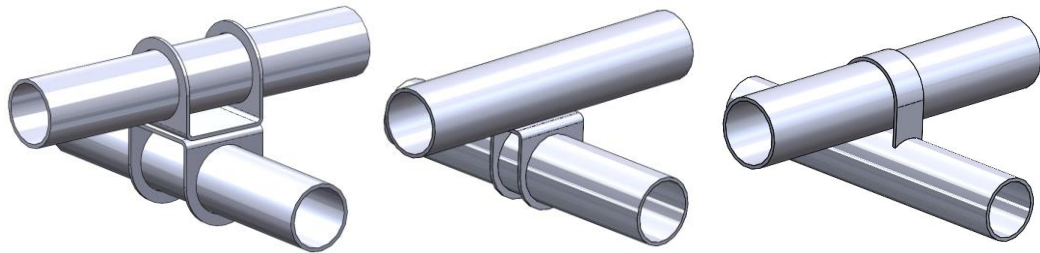


Figure 38. Alternative options for the joint of crossing tension rods.

The effect of different cornerplates between stiffeners was compared using FEA (figure 39).

The comparison was made with four configurations:

- No cornerplates
- 5 mm plates between stiffener webs
- 10 mm plates between stiffener webs
- 5 mm plates between stiffener flanges and webs

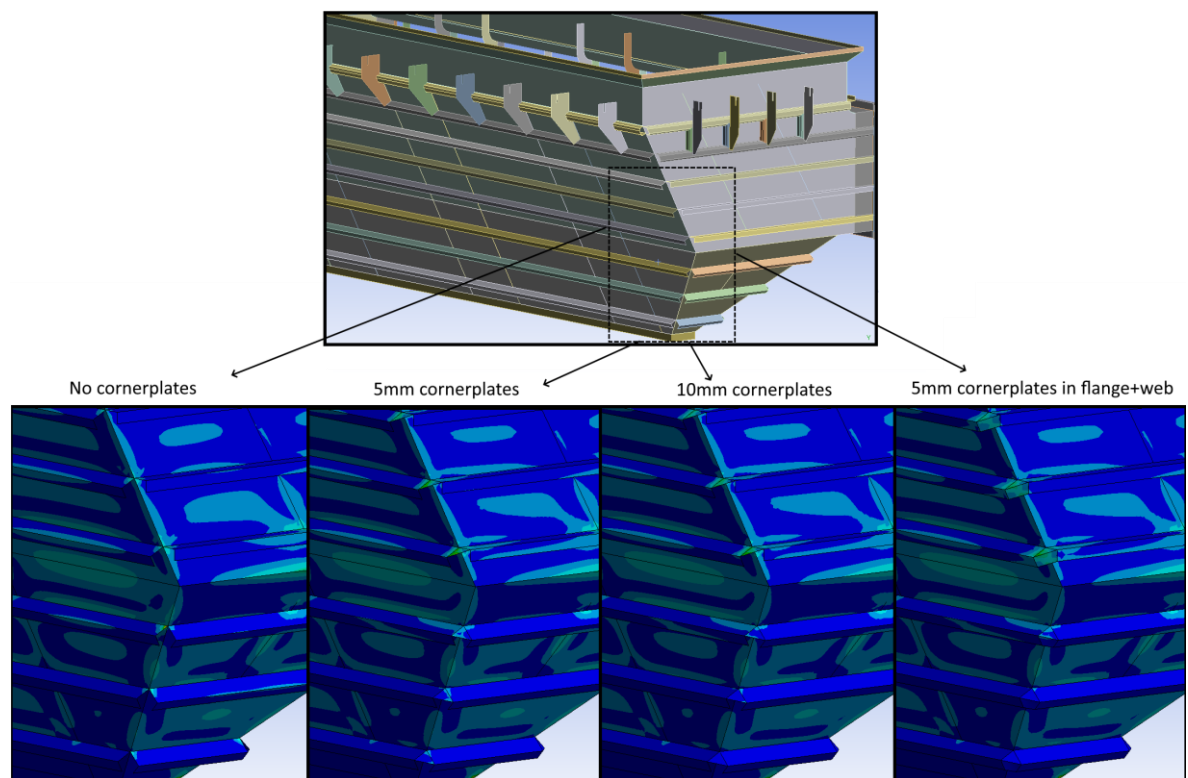


Figure 39. Von Mises stress of corner using different configurations.

From the results, it could be concluded that the cornerplates add rigidity of the corner, but the pyramidal hopper wall joints themselves are relatively rigid. The stress in the corner area is reduced by approximately 10-15% with the cornerplates. The highest benefit of the cornerplates is achieved if the joining plates are perpendicular to each other, like in flue gas

ducts. This effect can be seen by the stress distributions, on the top part of the hopper where the wall angles are closer to perpendicular, the stresses of cornerplates are much higher compared to the bottom pyramidal part. Respectively the amount of stress in corner joints between plates is vice-versa. The use of thicker cornerplates presumably reduces the stress in plates but 5 mm plates are adequate for the case. Cornerplate thickness at least equal to stiffener thickness can be generally considered adequate. Adding the cornerplates also between the flanges is extra work with not much structural benefit.

Attachment of the hopper and hangerplates were analyzed with FEA to create more efficient construction (figure 40). The von Mises stresses are low in the area of attachment while on the other hand there are peak stresses above the hangerplates so the design may be modified to be more efficient.

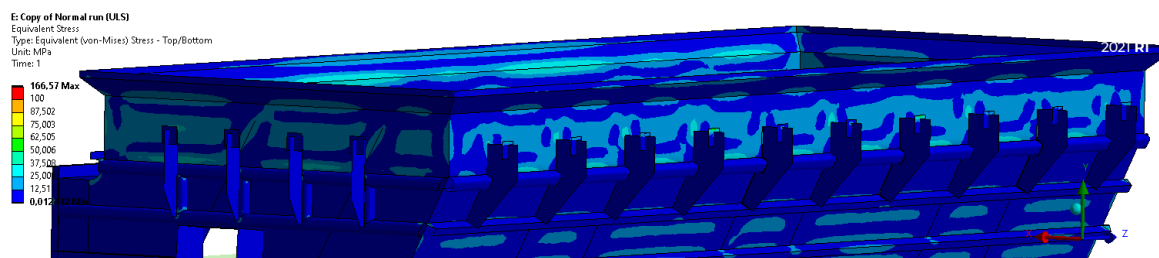


Figure 40. Von Mises stress of hopper in the area of attachment.

The thickness of hangerplates may be reduced and shape modified to allow for more efficient utilization. The number of hangerplates may be reduced and the placement of attachment beams is changed to allow for better support. Hangerplates should only be attached at sections where vertical stiffeners are located to allow for even stress flow through rigid supports. Placing the hangerplates in the unsupported part between stiffeners will cause considerable additional bending stress in the attachment plates due to flexing of the wall. Von Mises stresses of the corresponding case with modified attachment geometry is presented in figure 41. Stresses are more even across the area without increasing the peak stresses excessively.

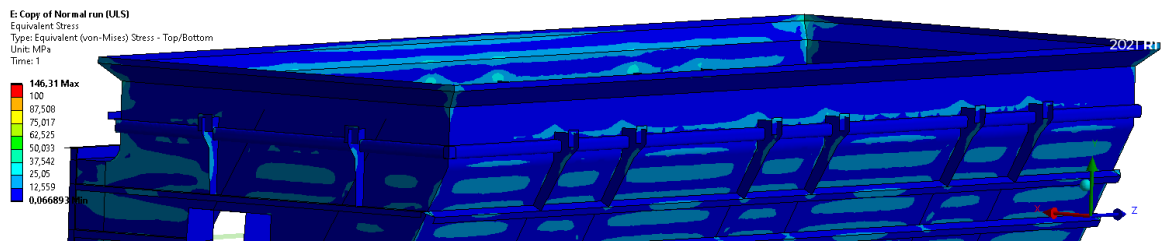


Figure 41. Von Mises stress of hopper in the area of attachment, modified geometry.

Turning on the large deflections for geometrically non-linear analysis did not alter the stresses of the structure in general. The deflections of the structure are relatively small, and this verifies the linear elastic behaviour.

6 DIMENSIONING TOOL

A general dimensioning tool is developed based on the presented theory and analysis of the reference hopper. The dimensioning tool is created in MS Excel. The tool is operated by inputting values or selecting options from dropdown menus and calculation is mostly automated. Calculation and dimensioning of the design is executed using the given theory and equations, but it is not shown in detail as the calculation process is hidden within the tool. Basic principles of the dimensioning process and functioning of the tool are presented along with FEA comparisons.

The dimensioning tool consists of 9 sheets:

- Guide page
- Geometry input
- Load data
- Material data
- Stiffener placement
- Tension rods
- Hopper loads
- Welds
- Summary

The design process starts by gathering all the required input data. General hopper dimensions are obtained by the layout design and wall plate thickness is an input parameter. Basic dimensions of the hopper are set as input to the dimensioning tool, and the hopper is divided into segments for calculation. Approximated plate areas and masses are calculated based on the geometry. Figure 42 presents part of the geometry input screen of the tool. Basic geometrical equations are used to define the wall panels for calculation and approximate the plate masses.

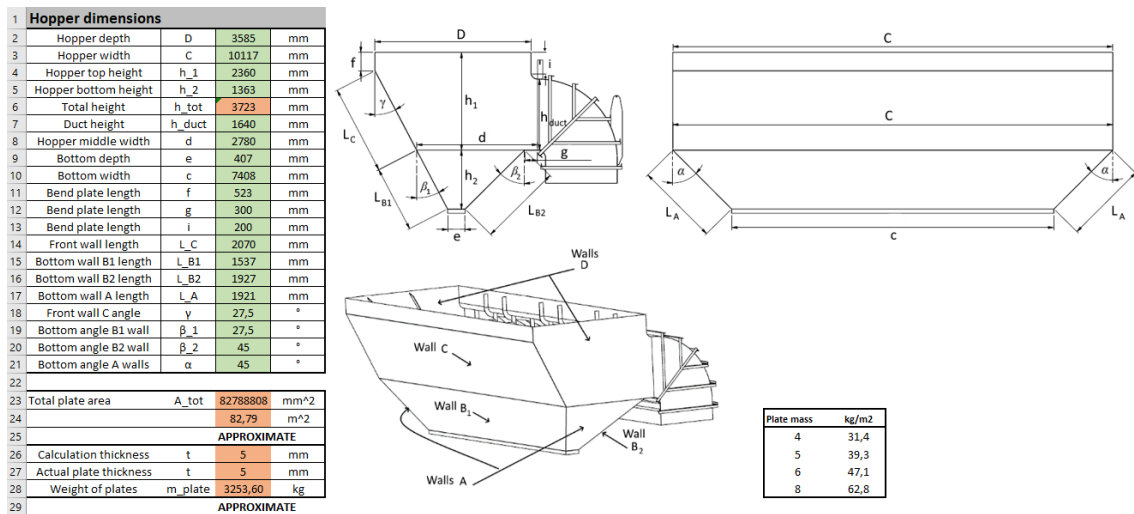


Figure 42. Geometry input for the dimensioning tool.

In addition to geometry, loads and material selection are set as input. The main load parameters are the ash density and flue gas pressure and then the tool calculates other variables such as pressure along the height of the hopper and total ash load while adding the partial safety factors. Materials for components are selected based on the flue gas temperature and the material parameters are automatically retrieved according to presented material tables (figure 43). Generally, it is recommended to select the highest strength material available while also considering the material cost and availability.

1	Input		
2	Flue gas temperature	T	400 °C
3	Design duration	t	10 000h
4			
5	Wall plate material		P265
6	Wall temperature		400 °C
7	Properties		
8	Yield strength at T	f _{y,T}	145,0 MPa
9	Ultimate strength at T	f _{u,T}	224,3 MPa
10	Creep strength	f _{u,c}	191,0 MPa
11	Design strength	f _{y,Ed}	145,0 MPa
12	Young's modulus at T	E _T	192000,0 MPa
13	Factor	B _w	0,9

Figure 43. Part of the material input and property screen.

The main focus of the tool is to determine the optimal layout of the stiffeners. Stiffener profile can be selected freely but the choice is aided by the tool to select the most efficient profile through total mass comparison. Stiffener cross-section properties are automatically calculated with the included effective width of the wall plate (figure 44).

1 Input			
2	Wall thickness	t	5 mm
3	Stiffener choice	Stiff_horiz	L 80x40x6
4			
5			
6 Material data			
14 Cross-section properties for ready profiles			
34 Calculation of cross-section properties for combination profile			
35	Area	A_stiff	692,2 mm ²
36	Second moment of area	I_stiff	483498,2 mm ⁴
37	Distance of NA	z_i	51,2 mm
38	height	h_stiff	80 mm
39	thickness	t_stiff	6 mm
40 Wall plate with EN 1993-1-4 effective width			
41	Yield strength	f_y	235 Mpa
42	epsilon	e	1
43	effective width factor	n_ew	15
44	Area	A_plate	750 mm ²
45	Second moment of area	I_plate	1562,5 mm ⁴
46	Distance of NA	z_i	2,5 mm
47	Eff. width on each side	B_eff	75 mm
48 Combination profile			
49	Area	A_prof	1442,2 mm ²
50	Position of NA	z_NA	25,87 mm ⁴
51	Second moment of area	I_prof	1338800,03 mm ⁴
52	Max distance from NA	c	59,13 mm
53	Section modulus	W	22643,21 mm ³
54	Statical moment	Q	17530,58 mm ³

Figure 44. Calculation of cross-section properties.

Recommended dimensions for plate segments and stiffener placement are calculated based on the allowable stresses in plates and stiffeners and the optimal b/a -ratio is iterated as described earlier. The maximum distance between horizontal stiffeners is reduced towards the bottom of the hopper according to the increased ash load. The tool generates the recommended dimensions for vertical and horizontal stiffener placement along with automatic visualization for individual wall panels to easily check the results (figure 45). Stiffeners are placed on the wall panels based on the maximum dimensions and geometrical constraints.

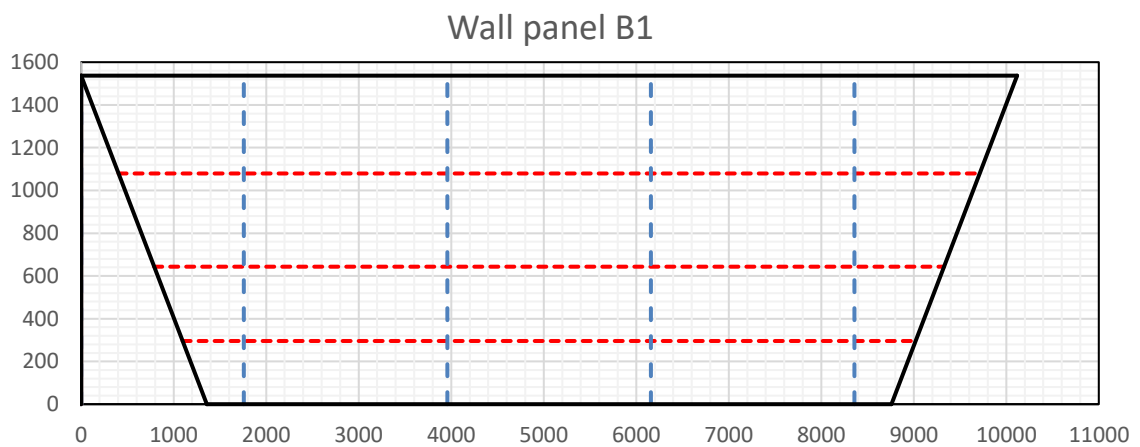


Figure 45. Dimensioning tool visualization of stiffener layout for the example wall panel.

Analytical dimensioning tool results were compared against FEA results with the example hopper. Example material set for the wall panels and vertical stiffeners is P265 so the corresponding design strength at temperature is 145 MPa and the selected material of horizontal stiffeners is S355 so the corresponding design strength at temperature is 120 MPa. Load case 1 is used in the analysis as it is the determinative case for stresses and deformations. Figures 46 and 47 present the hopper dimensioned with the developed design tool and von Mises stresses verified with FEA. Figure 48 presents the corresponding total deformation. The maximum stress in a plate segment is approximately 120 MPa and in a horizontal stiffener 110 MPa. The stresses are well below the design strengths with the recommended stiffener placement by the dimensioning tool, while providing quite even stress distribution.

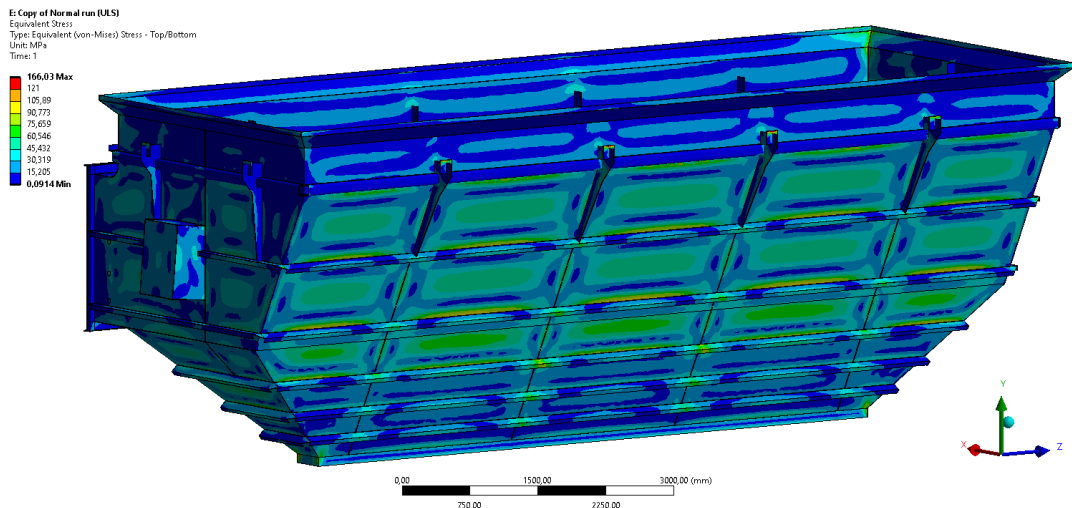


Figure 46. Global stresses of verified using FEA, front of the hopper.

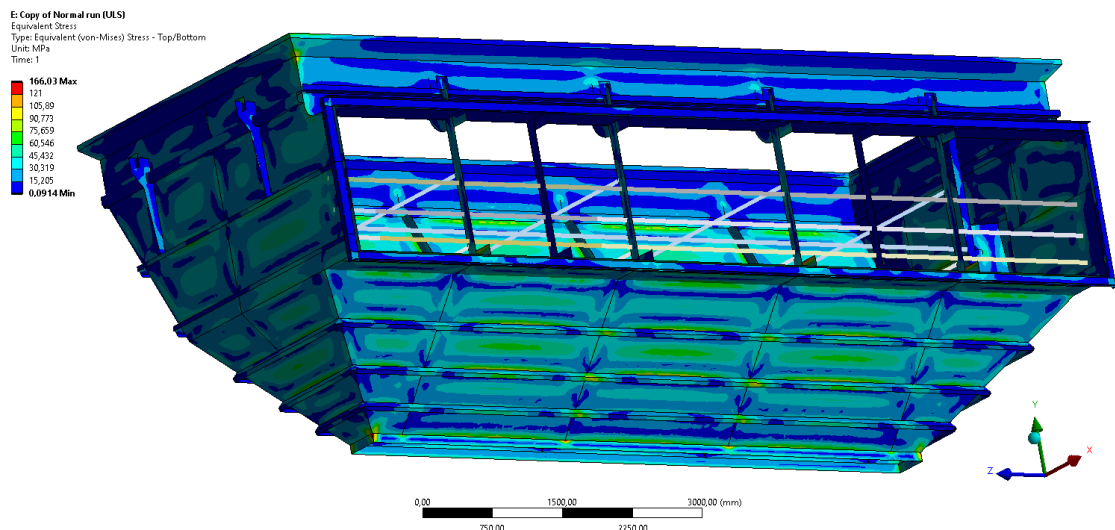


Figure 47. Global stresses verified using FEA, rear of the hopper.

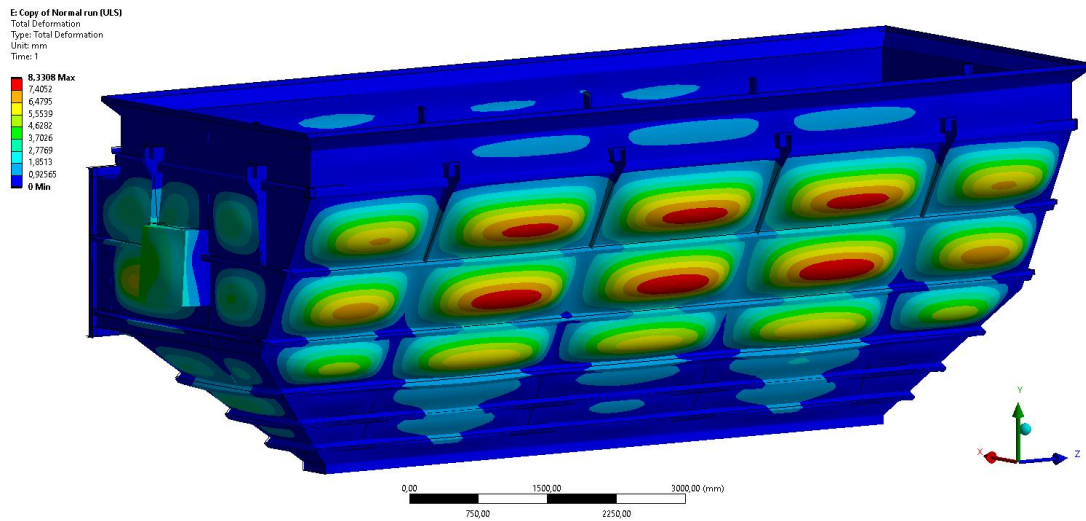


Figure 48. Global total deformations with FEA.

Tension rods are placed to support walls in general and limit the local stresses. The calculation method for estimating the internal forces of the tension rods presented in SFS-EN 1993-4-1 did not turn out to be accurate for the hopper due to the angled walls and forces being distributed unevenly. Tension rod forces are estimated manually according to equation 26. Rod forces between the dimensioning tool and FEA (figures 49 and 50) are compared in table 14. Rod forces are studied at different levels near the center of the hopper as the maximum forces are present there. Tension and buckling resistance of individual rods is checked based on the presented equations and adequate profile is chosen.

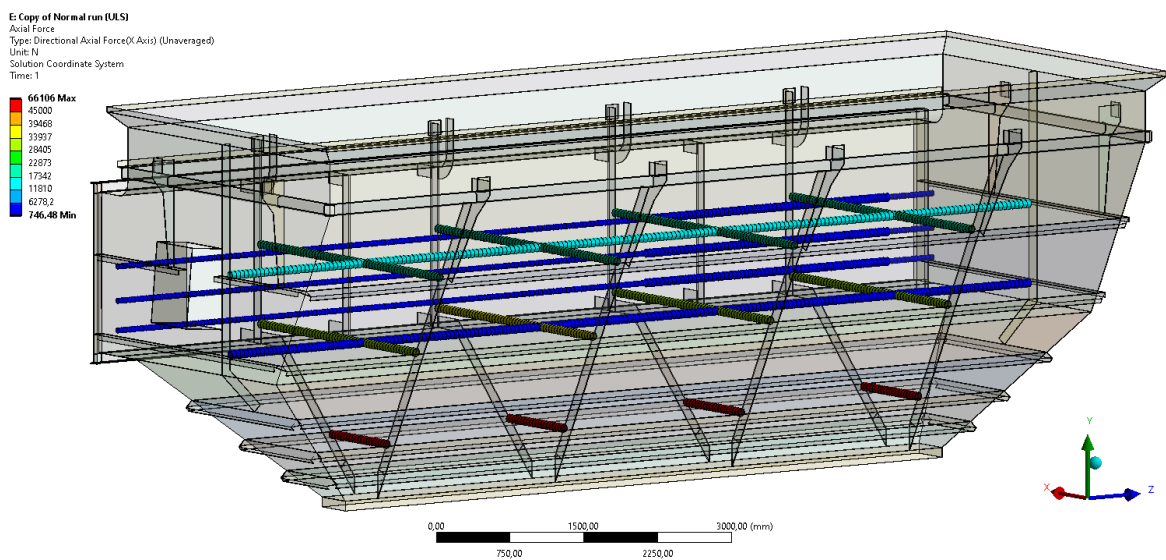


Figure 49. Tension rod axial forces, LC1.

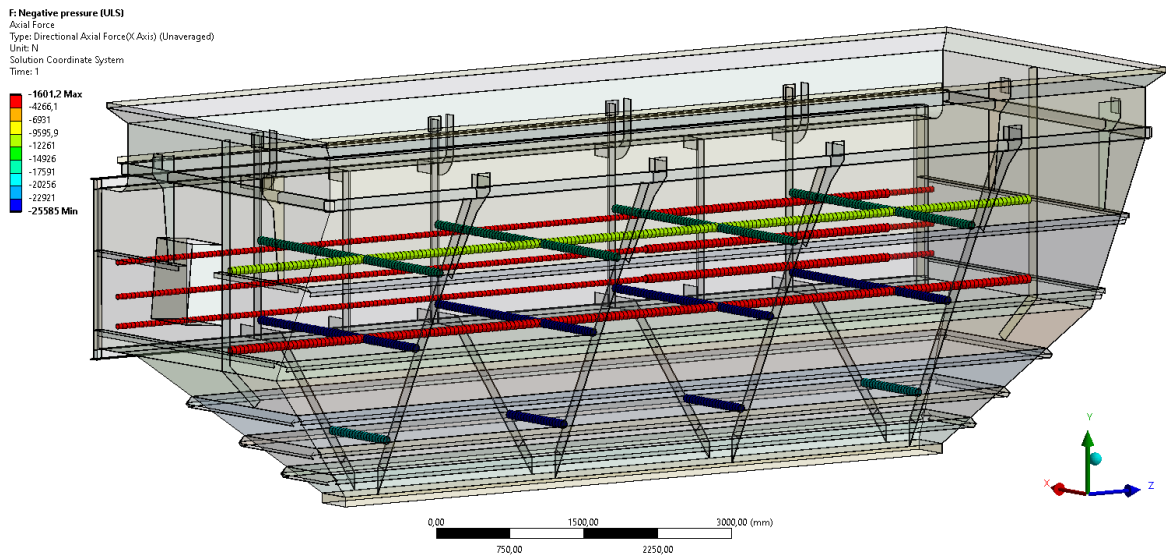


Figure 50. Tension rod axial forces, LC2.

Table 14. Comparison of tension rod forces by analytical methods and FEA.

Rod ID	LC 1 Axial force			LC 2 Axial force		
	Analytical tool [kN]	FEA [kN]	Difference [%]	Analytical tool [kN]	FEA [kN]	Difference [%]
1	71.1	66.1	+7.6	-27.9	-25.8	+8.1
2	25.1	33.2	-24.7	-20.5	-25.3	-19.0
3	16.4	18.7	-12.3	-16.4	-13.6	+20.5

The simple analytical calculation of tension rod forces provides a rough estimation of the true forces. Tension rod forces are highly dependent of the locations in the wall and rod pressure areas require estimation. The tool gives a good baseline for the selection and placement of tension rods, but more accurate methods should be used for verification.

The last sheets of the dimensioning tool provide an estimation of the attachment loads and aid the dimensioning of welds. The sheet “hopper loads” gathers all the weights of components and estimates the vertical reaction forces of the attachment plates. Reaction forces should be only used as a reference as the possible additional bending stresses due to pressures in the walls cannot be analytically considered easily and accurately. The calculation sheet “welds” provide ready equations for the main weld joints of the hopper. Weld dimension requirements are also presented and checked.

Most of the calculation in the tool is executed automatically based on the given input data. This lowers the risk of user error. There is also some error detection implemented into equations and user can quickly check the visual results. The user of the tool must be familiar with the design criteria to be able to assess the validity of the results. The tool provides a good baseline for the design, especially for the placement of stiffeners and the calculation of tension rods. However, certain design details like the attachment need to be manually considered and checked.

Dimensioning tool does not include plate buckling as the buckling is not considered to be a critical failure mode, but simple linear buckling analysis was done by FEA to verify global stability with negative flue gas pressure. The lowest linear buckling load multiplier is 8.9 (figure 51). The linear multiplier is considered adequate and reduced buckling capacity is not calculated in detail as it is not considered in this thesis.

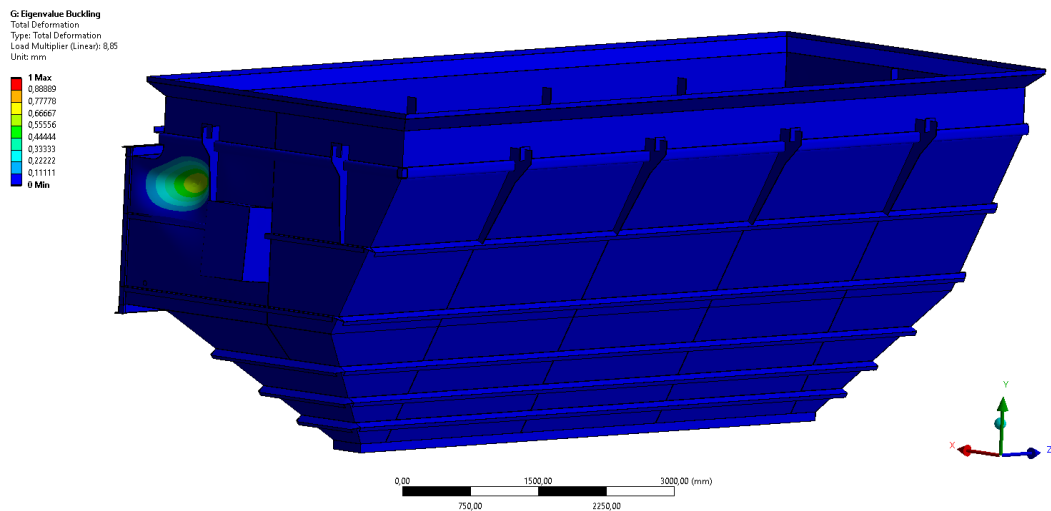


Figure 51. Lowest linear buckling mode, load case 2.

7 DISCUSSION

Defining the design criteria, methods and load cases is a crucial step before the analysis. The importance of certain factors and their effects on the design are discussed along with the used analysis methods. The design was optimized by applying design criteria, and dimensioning tool was created based on the set strength requirement. The functionality of the tool and its effect on the design process is shortly discussed. Lastly, future development ideas are presented along with alternative design options.

7.1 Most important factors defining the design and analysis

There are no direct standards or rules that would explicitly set general design requirements for an ash hopper. The designer of the equipment is responsible for setting the requirements and load cases so the structure can withstand all the possible situations along its lifetime with sufficient safety. Part of the Eurocode standards can be used as guidelines for the criteria and calculation methods.

As with all boiler components, temperature is one of the most important factors to be considered in the design. It lowers the nominal strength of the material, can introduce creep and it affects the stability of members. Defining the corresponding material properties by the correct flue gas temperature is important for the analysis. Especially the structural steel properties are not uniform across different standards. Strength values presented by SFS-EN 13084-7 are significantly lower than obtained by the temperature models from fire design standard SFS-EN 1993-1-2. Lower values from SFS-EN 13084-7 are used in the calculation as the silo design standard recommends the use. More capacity of the material could possibly be utilized if the higher strength values are justified. Practical material tests show that fire design standard reductions correspond well to the actual material behavior with S355 and S420 steels. Actual strength values are even slightly higher than standard values. (Outinen 2006, pp. 237-251.) However, possible creep phenomena is not considered as long exposure testing was not conducted. Whether it is even relevant to consider creep explicitly in ash hoppers is also an aspect that can be only confirmed by practical testing. Actual flue gas temperature and true loads subjected to the hopper vary throughout the lifetime of the boiler and are not constantly high.

The thermal stresses can be efficiently eliminated by good insulation and allowing thermal elongation. The temperatures of the hopper were assumed to be relatively even based on previous analyses. Additional thermo-structural analysis was therefore not conducted in this thesis.

Defining the load cases is an important aspect in the analysis. Process parameters define the flue gas pressure and temperatures and the highest possible amount of ash accumulating in the hopper should be considered. Justification of the interaction between the maximum load components was an important concern. Load cases should include all the possible situations but optimally should not be overly conservative. By using partial factors, some uncertainties of loads are already included.

Simplifications were made to ease the analysis and to make it possible by analytical methods. Silo load components were replaced by simple hydrostatic pressure load as it gives equal or more conservative approximation with less effort. The stress of a single stiffened plate and stiffener in a continuous plate can be calculated with reasonable accuracy using basic strength of materials. Only linear-elastic analysis methods are utilized in this thesis. It is relatively simple and easily applicable for an analytical dimensioning tool. However, the true capacity of the hopper is considerably higher if plasticity capacity is also included. Non-linear methods could be used to justify further utilization of the design.

7.2 Design optimization

The design was optimized by practical engineering approach, comparing different options and their estimated effect on the total mass and manufacturing costs. General design details were assessed with FEA of the general hopper structure. Construction of the hopper attachment was slightly altered to reduce mass, welding and allow for more even stress flow. Hangerplate geometry can also be modified to reduce weight and the number of plates reduced depending on the case. Welding and cutting of tension rods is drastically reduced by changing to separate connectors. Different weld joints were examined and required throat thicknesses of joints calculated to reduce the total amount of welding. The effect of plate thickness on the total cost of manufacturing was researched with simple comparisons. Thicker plates reduce the amount of welding and use of stiffeners but increase in total mass

outweighs the gained benefits. Thinner plates provide the lightest structure resulting in a more cost-efficient design.

Defining the layout and profile of stiffeners was the main interest of the tool as defining it with FEA usually requires manual work and iteration. An iterative solver for finding the b/a -ratio with the plate stress and stiffener stress equal and below design strength was developed. With linear calculation, the principle seems to be functional and provide an efficient solution.

Challenge was to optimize the design in general. Details for the specific studied hopper could easily be tested and compared with FEA. The problem is to come up with design rules for the details ensuring that they are applicable to all hoppers as well. For detailed optimization of a specific hopper, separate FE-analysis should be conducted, but the dimensioning tool and design guide provide a good baseline for the design. The final optimal solution is a balance between components as different details affect each other.

7.3 Dimensioning tool

Based on the analysis of hopper design, the goal was to create a dimensioning tool to easily define the basic design of the hopper. Multiple options for the tool were initially considered, such as Excel or Mathcad calculation sheet, design tables or parametric FE-model. MS Excel is available to all and easy to use but also has decent calculation capacity, so it was chosen as the platform for the tool. Parametric FE-model would be the most accurate solution, but it is complex as it requires more configuration and also interpretation of the results.

The goal was to implement all parameters as easily changeable variables so different effects could be examined. This was achieved greatly, and the tool is easily customizable for tuning and testing. The tool simplifies and makes the design process faster, as most of the design variables are automatically obtained after inputting the required values. It is suitable for hoppers that have a similar design and is applicable for all sizes of hoppers. The tool does not fully automate the design process as there are always details that need to be determined manually. The tool and general conclusions presented in this thesis guide the design of details. There is well amount of total safety by the used load partial factors, material data, methods, and assumptions but the tool user needs to be conscious and familiar with the hopper design criteria. The dimensioning tool should be further tested in future projects along

with FEA comparison to verify the accuracy of made assumptions in special cases. Considering all the local phenomena only using simplified analytical calculation is not easily and accurately possible in all cases.

7.4 Future development

Dimensioning tool has good potential to help and make the design process faster. Currently, the tool only covers one type of hopper geometry, but it can be updated in the future to be applicable in different configurations and possibly other structures involving stiffened panels. All the basic geometry data is inputted into the tool and placement of stiffeners is given, so the tool could be further developed into an automatic design configurator. The tool will also be developed further, and the calculation routine refined.

This thesis only focused on one type of ash hopper and the design was not radically changed from the original. The current design has been proven to be functional and relatively efficient, so for simplicity, the design was mostly kept unchanged. The focus was to study the current configuration and optimize its details. The design could be further enhanced by totally changing the design or its features.

The design of the ash hopper is driven by structural strength requirements and deflections are not a major limitation. Therefore, it is beneficial to use high-strength materials. Higher strength steels do not offer an advantage against deformation but allow for higher stress levels. The presented material selection is mostly based on material resistance to temperatures and available material properties at elevated temperatures. Expanding the selection of structural steels beyond S355 could be beneficial as the amount of stiffening or plate thicknesses may be reduced. Other relevant higher strength steels could also be utilized according to their resistance to temperature.

The challenge is the lack of available material data at elevated temperatures. Eurocodes do not present tested elevated temperature material properties of structural steels beyond S355-grade or for other similar steels. Fire design standard presents reduction models for high-temperature strength values which are applicable up to S460 structural steels. Other international standards also provide material properties in high temperatures, but this thesis focused on the EN standards. Material usage in high temperatures cannot be justified without testing

or reliable material data. Availability of materials can also be the determining factor, as the hoppers are manufactured by subcontractors in different locations. Plates with higher strength are often easily available but for profiles, the material selection is more limited.

The use of curved shell profiles as walls would greatly increase the load-bearing capacity as the curved shapes could withstand the loads by membrane stresses. Curved shapes would however lead to very challenging manufacturing and assembly. Due to joining structures, like the flue gas duct and attachment to the backpass, the circular shapes are practically impossible to implement.

Ready-made profiles are used as stiffeners because they are readily available and relatively cheap. Different profiles are well suitable for stiffening purposes, but the most optimal solution would be achieved with custom stiffeners. Trapezoidal shape (figure 52) is generally the best shape for stiffener as it offers great stiffness and customizability. Trapezoidal profiles are not generally available, so they would need to be manufactured. They can offer optimum stiffening solution but also introduce additional challenges. With trapezoidal stiffeners, additional local effects should be considered due to the attachment of tension rods in the unsupported part. Local buckling of stiffener plates should also be taken into consideration. The trapezoidal shape also forms a closed profile with the plate wall, and therefore it complicates the insulation of the hopper.

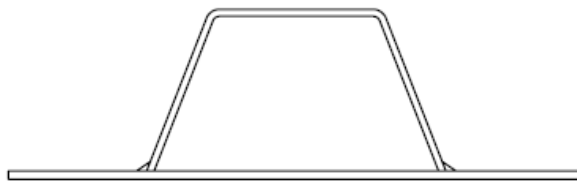


Figure 52. Trapezoidal stiffener welded to a plate.

Another option for stiffening would be incorporating the stiffeners into the plates by using corrugated panels. This way the stiffeners at least in one direction could be eliminated and welding reduced. Corrugations should be oriented in the flow direction of ash so the ash would not accumulate in the pockets. Corrugated panels however would set more challenges in the manufacturing and assembly of the hopper.

An alternative option for stiffened plates could be a steel sandwich plate. A sandwich plate is a construction where 2 parallel plates are joined together by the inside stiffening structures (figure 53). With sandwich plates, the external stiffening and related welding could be minimized or eliminated altogether. Sandwich plates also allow for customization in materials, as different parts of the construction can be made from different materials. For example, the inside wall of the hopper could be made from more wear- and heat-resistant material as it is in direct contact with ash particles and flue gas. The downside to the use of sandwich plates is again that it sets additional challenges in wall joints and in the attachment of surrounding structures. Heat conduction properties of the sandwich plates and behavior in temperatures should also be researched.

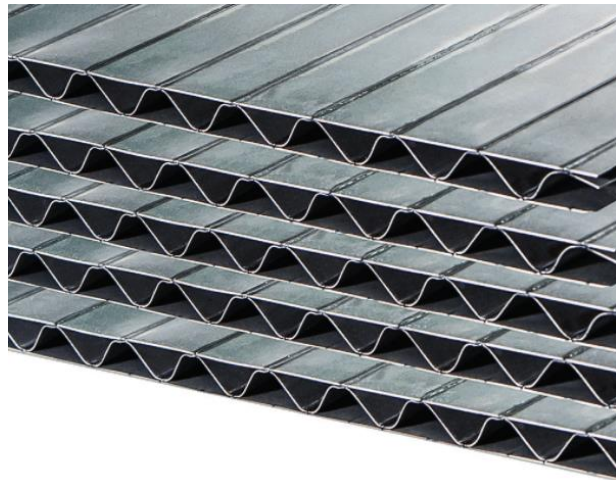


Figure 53. Steel sandwich plates (HT Laser 2021).

8 CONCLUSION

Unlike for the pressure parts, there are no direct standards for the design and requirements of ash hoppers in boilers. The designer and supplier is responsible for ensuring the safety and functionality of the equipment. Part of EC3 can be used in defining the guidelines for the hoppers along with principles from the strength of materials. The design requirements were set by assessing possible failure modes of the structural members by utilizing limit state design.

The hopper structure was analyzed and optimized primarily using FEA. Different constructions and options were compared to find the best solution. Certain design details were enhanced by reducing unnecessary material and by alternative constructions. The analysis was based on one specific hopper and conclusions are applicable in general, but certain details should always be considered case-by-case. FEA of the whole ash hopper structure is the recommended analysis method but analytical calculation methods were needed for the MS Excel-based hopper dimensioning tool. Stiffened plates are analyzed by dividing the plate into individual segments and calculating the stresses of plates and stiffeners. Different calculation methods were compared to verify the accuracy of simplified methods. The use of hydrostatic pressure as an ash load was validated to be applicable instead of complex silo load components.

The developed dimensioning tool can be used to define the basic design parameters for an ash hopper. Determining the stiffener layout for the hopper walls was the primary parameter to be solved and an iterative calculation routine was created to define the maximum plate segment dimensions with a specific stiffener profile and automatic recommended placement on the walls. The dimensioning tool has potential to speed up the design process as it defines most parameters automatically, but manual consideration is needed in the design.

This thesis only focused on linear-elastic calculation, but the design could be further exploited by utilizing the plastic capacity and non-linear analyses. Hopper design also was not radically changed from the original but alternative constructions or materials could potentially improve the design.

LIST OF REFERENCES

Bhaskar, K. Varadan, T.K. 2021. Plates - Theories and Applications. Cham: Springer. 282 p.

González-Velázquez, J.L. 2020. Mechanical Behavior and Fracture of Engineering Materials. Structural Integrity, Vol. 12. Cham: Springer. 244 p.

Gunalan, S. Heva, Y.S. Mahendran, M. 2014. Flexural - torsional buckling behaviour and design of cold-formed steel compression members at elevated temperatures. Engineering Structures, Vol. 79. Elsevier Ltd. pp. 149-168.

HT Laser 2021. [Online image] [Referred 25.10.2021] Available: <http://www.teraskennolevy.fi/>

Kassner, M.E. 2009. Fundamentals of creep in metals and alloys. 2nd edition. Elsevier Ltd. 288 p.

Outinen, J. 2006. Mechanical properties of structural steel at elevated temperatures and after cooling down. Fire and Materials, Vol. 28: 2-4. John Wiley & Sons Ltd. pp. 237-251.

NFPA 85. 2019. Boiler and Combustion Systems Hazards Code. Massachusetts: National Fire Protection Association. 240 p.

Niemi, E. 2003. Tekninen tiedotus 2. Levyrakenteiden suunnittelu. Helsinki: Teknologiateollisuus ry. 136 p.

Niemi, E. Kemppi, J. 1993. Hitsatun rakenteen suunnittelun perusteet. 337 p. Helsinki: Opetushallitus.

Salmi, T. Pajunen, S. 2018. Lujuusoppi. Tampere: Pressus Oy. 462 p.

SFS-EN 1990. 2002. Eurocode. Basis of structural design. Helsinki: Finnish Standards Association SFS. 89 p.

SFS-EN 1991-1-4. 2007. Eurocode 1. Actions on structures. Part 4: Silos and tanks. Helsinki: Finnish Standards Association SFS. 109 p.

SFS-EN 1993-1-1. 2005. Eurocode 3. Design of steel structures. Part 1-1: General rules and rules for buildings. Helsinki: Finnish Standards Association SFS. 98 p.

SFS-EN 1993-1-2. 2005. Eurocode 3: Design of steel structures. Part 1-2: General rules. Structural fire design. Helsinki: Finnish Standards Association SFS. 82 p.

SFS-EN 1993-1-3. 2006. Eurocode 3. Design of steel structures. Part 1-3: General rules. Supplementary rules for cold-formed members and sheeting. Helsinki: Finnish Standards Association SFS. 132 p.

SFS-EN 1993-1-5. 2006. Eurocode 3. Design of steel structures. Part 1-5: Plated structural elements. Helsinki: Finnish Standards Association SFS. 55 p.

SFS-EN 1993-1-7. 2007. Eurocode 3. Design of steel structures. Part 1-7: Plated structures subject to out-of-plane loading. Helsinki: Finnish Standards Association SFS. 38 p.

SFS-EN 1993-1-8. 2005. Eurocode 3. Design of steel structures. Part 1-8: Design of joints. Helsinki: Finnish Standards Association SFS. 138 p.

SFS-EN 1993-4-1. 2007. Eurocode 3. Design of steel structures. Part 4-1: Silos. Helsinki: Finnish Standards Association SFS. 116 p.

SFS-EN 1993-4-1/AC. 2009. Eurocode 3. Design of steel structures. Part 4-1: Silos. Helsinki: Finnish Standards Association SFS. 4 p.

SFS-EN 10028-2. 2017. Flat products made of steels for pressure purposes. Part 2: Non-alloy and alloy steels with specified elevated temperature properties. Helsinki: Finnish Standards Association SFS. 32 p.

SFS-EN 13084-7. 2013. Free-standing chimneys. Part 7: Product specifications of cylindrical steel fabrications for use in single wall steel chimneys and steel liners. Helsinki: Finnish Standards Association SFS. 26 p.

SFS 3052. 2020. Welding vocabulary. General terms. Helsinki: Finnish Standards Association SFS. 128 p.

Valmet MyAcademy [internal database]

Creep properties of pressure grade steels (SFS-EN 10028-2, pp. 20-22).

Steel name	Steel number	Temperature [°C]	Strength for 1% plastic creep strain [MPa]		Creep rupture Strength [MPa]		
			10 000h	100 000h	10 000h	100 000h	200 000h
P235GH P265GH	1.0345 1.0425	380	164	118	229	165	145
		390	150	106	211	148	129
		400	136	95	191	132	115
		410	124	84	174	118	101
		420	113	73	158	103	89
		430	101	65	142	91	78
		440	91	57	127	79	67
		450	80	49	113	69	57
		460	72	42	100	59	48
		470	62	35	86	50	40
		480	53	30	75	42	33
P355GH	1.0473	380	195	153	291	227	206
		390	182	137	266	203	181
		400	167	118	243	179	157
		410	150	105	221	157	135
		420	135	92	200	136	115
		430	120	80	180	117	97
		440	107	69	161	100	82
		450	93	59	143	85	70
		460	83	51	126	73	60
		470	71	44	110	63	52
		480	63	38	96	55	44
		490	55	33	84	47	37
		500	49	29	74	41	30
16Mo3	1.5415	450	216	167	298	239	217
		460	199	146	273	208	188
		470	182	126	247	178	159
		480	166	107	222	148	130
		490	149	89	196	123	105
		500	132	73	171	101	84
		510	115	59	147	81	69
		520	99	46	125	66	55
		530	84	36	102	53	45

APPENDIX I,2

Creep properties of pressure grade steels (SFS-EN 10028-2, pp. 20-22).

Steel name	Steel number	Temperature [°C]	Strength for 1% plastic creep strain [MPa]		Creep rupture Strength [MPa]		
			10 000h	100 000h	10 000h	100 000h	200 000h
13CrMo 4-5	1.7335	450	245	191	370	285	260
		460	228	172	348	251	226
		470	210	152	328	220	195
		480	193	133	304	190	167
		490	173	116	273	163	139
		500	157	98	239	137	115
		510	139	83	209	116	96
		520	122	70	179	94	76
		530	106	57	154	78	62
		540	90	46	129	61	50
		550	76	36	109	49	39
		560	64	30	91	40	32
		570	53	24	76	33	26
10CrMo 9-10	1.7380	450	240	166	306	221	201
		460	219	155	286	205	186
		470	200	145	264	188	169
		480	180	130	241	170	152
		490	163	116	219	152	136
		500	147	103	196	135	120
		510	132	90	176	118	105
		520	119	78	156	103	91
		530	107	68	138	90	79
		540	94	58	122	78	68
		550	83	49	108	68	58
		560	73	41	96	58	50
		570	65	35	85	51	43
		580	57	30	75	44	37
590	50	26	68	38	32		
600	44	22	61	34	28		